

1 **Influence of Aggressive Exposure on the Degradation of Nano-Silica**
2 **Admixed Cementitious Mortar Integrated with Phase Change Materials**

3

4

5

6

7

8

9

10

11

12 Snehal K¹ and B B Das^{1*} and Salim Barbhuiya²

13

14

15

16

17

18

19

20

21

22

23 ¹Department of Civil Engineering, National Institute of Technology Karnataka, Surathkal,
24 Karnataka, India, 575 025.

25 ²Department of Engineering and Construction, University of East London, United
26 Kingdom

27 *Corresponding Author

28 **Abstract:**

29 The objective of the present study is to evaluate the stability of cementitious mortar
30 incorporated with phase change material (PCM, n-octadecane) at aggressive exposure
31 conditions such as acid (1% H₂SO₄), alkali (5% Na₂SO₄) and chloride (5% NaCl).
32 Thermogravimetric analysis (TGA) was performed to characterize and quantify the amount
33 of deleterious compounds such as ettringite (Ca₆Al₂(SO₄)₃(OH)₁₂·26H₂O, AFt), gypsum
34 (CaSO₄·2H₂O Gy) and Friedel's salt (Ca₂Al(OH)₆(Cl, OH)·2H₂O, Fs) formed due to the
35 action of SO₄²⁻ (acidic and alkaline media) and Cl⁻ (chloride media) ions at the continuous
36 exposure period of 180 days. Mass loss associated to the thermal degradation of n-
37 octadecane PCM (CH₃(CH₂)₁₆CH₃) at various exposure solutions was also calculated at the
38 temperature boundary of 250-300 °C. This study also highlights the introduction of
39 optimized nano-silica dosage (3%) into the PCM based cementitious mortar to counteract
40 the undesirable facets of PCMs on cementitious system.

41 Results revealed that incorporation of PCM in cementitious mortar augmented the amount
42 of AFt, Gy (at acid and alkali exposure solution) and Fs (at chloride exposure solution)
43 formation, responsible for the amplified rate of deterioration. It is important to be noted
44 that after long term exposure of 180 days no traces of PCM was observed in PCM based
45 cementitious mortar mixes, which signifies the mixes no longer holds the capacity to store
46 energy. However, co-occurrence of nano-silica (3%) in PCM based cementitious mixes
47 curtailed the negative impact of PCM on cementitious mortars exposed to aggressive
48 conditions significantly. Further, differential thermogravimetric (DTG) curve shows an
49 additional endothermic peak at 250-300 °C for 3% nano-silica modified PCM based
50 cementitious mixes even after exposure to aggressive ions that implies the ability of the
51 mix to sustain the thermal efficiency characteristics of PCMs.

52 **Key Words:** Phase change material (PCM), nano silica, aggressive ions, durability, length
53 change.

54

55 1. Introduction

56 Rapid growth in industrialization and urbanization significantly increased the consumption
57 rate of energy. Building and infrastructures are considered to be one of the leading
58 consumers of energy. Major part of the energy consumed in commercial and residential
59 buildings is for maintaining thermal comforts of habitants i.e. especially for space
60 conditioning and heating. Current estimation says that more than 50% of the global energy
61 is being spent at space cooling and heating in building sectors [1-2]. This necessitates the
62 need for conservation of energy and to improve the energy efficiency of the buildings and
63 infrastructure. In this point of view, thermal energy storage and latent heat storage systems
64 are gaining importance for various developments in energy conservation [3-4]. Phase
65 change materials (PCMs) are one such novel sensible and latent heat storage materials
66 which has an ability to absorb and dissipate heat when the material changes its phase from
67 solid to liquid and vice versa [4-6]. PCMs can be incorporated in to a number of
68 construction materials such as gypsum boards, masonry wall with bricks, concrete, asphalt
69 etc., [7-8]. Concrete/cementitious composites are widely used global construction material,
70 which are porous in nature and acts as an ideal media for PCMs incorporation [5-6, 9-10].
71 Utilization of PCMs in cementitious composites has gained lot of attention by the research
72 community to minimize the energy loading in buildings.

73 Various types of PCMs can be incorporated in concrete/mortar using different techniques
74 [7, 11]. Among several PCMs, organic types are most preferred by the researchers owing
75 to its better stability in cementitious system [7-8]. N-octadecane is one such organic PCMs
76 which has potential ability to store latent heat and can withstand larger thermal cycles [6,
77 11]. Major detriment of PCMs use in cementitious composites is loss in structural integrity
78 owing to its leakage issue [5, 9]. This is found to be as foremost limitation for its structural
79 utility. It is also reported that incorporation of PCMs in cementitious composites are
80 responsible for increase in permeable porosity [10, 12]. PCM presence in cementitious
81 system adversely affects the strength and durability performance of cementitious
82 composites [9, 12]. From the literature it is understood that most of the studies on PCM
83 based cementitious mortar/concrete were concentrated on the influence of PCMs on
84 thermal and mechanical aspects of cementitious composites [6-7, 11 13-14]. It is reported
85 that addition of PCMs reduces mechanical strength [6, 11, 13], disturbs the hydration

86 process [5, 9] and increases the porosity [6, 10, 12] of cementitious composites. Further,
87 studies stated that incorporation of PCMs in cementitious composites enhances the
88 specific/latent heat [6, 14-18] and reduces the thermal conductivity [15-17].

89 In the present scenario, another important deciding parameter for any structural material is
90 that its **response** against aggressive environment. Country like India encompasses varied
91 weather conditions with vast coastal area in the south. Aggressive change in climatic
92 condition is triggered by means of speedy evolution of industries and cities over the period
93 of time. This dramatic change in climatic condition is always been a concern in regard to
94 the service life of concrete/cementitious composites. From various studies it is evident that
95 cementitious composites deteriorates and loses its structural properties on exposing to
96 aggressive conditions [19-20]. Wei et al (2017) reported that significant reduction in
97 enthalpy (**of the order 25%**) was experienced when PCM based cementitious composite are
98 exposed to **sulfate** bearing environment. However, very limited studies are focused on the
99 durability aspect of PCM incorporated cementitious composites against aggressive ions
100 [21].

101 **Sulfate** (SO_4^{2-}) and chloride (Cl^-) are the major detrimental aggressive ions that impacts the
102 service life of cementitious composites [19]. **Sulfate** attack in the form sulfuric acid (acidic)
103 and **alkaline (Na, K, Mg) sulfate** are responsible for the formation of expansive compounds
104 such as gypsum (Gy) and ettringite (AFt) which hampers the cementitious system [20].
105 Similarly, cement based concrete or mortar also have least resistance to chloride attack. It
106 is reported that continuous exposure of cementitious composites to chlorides may cause
107 deleterious effects such as a) decalcification of calcium hydroxide resulting leaching of
108 calcium chloride, b) development of porous C-S-H and c) formation of voluminous
109 compound such as Friedel's salt and its analogous due to the reaction between calcium
110 aluminates and chloride ions, ultimately leading to cracks in concrete [22]. At this point of
111 time, it is very much essential to study the durability parameters of the innovative smart
112 cementitious composite composing of PCM under different aggressive exposure conditions
113 such as acidic, alkaline and saline media.

114 On the other hand, the concept of nanotechnology to improve the performance of
115 cementitious composites by making use of nano-sized materials has opened up a new drive

116 in concrete history. Nano-silica, a silica enriched nano particle (with active SiO₂ content
117 >99.5%) is the most preferred nano-scale material in cementitious composites as a
118 performance enhancing ingredient [23]. Nano-silica is considered to be as superior
119 pozzolanic ingredient with a potential to boost the extent of chemical reactivity owing to
120 its high surface to volume ratio [24-25]. It was reported that incorporation of small
121 percentage of nano-silica in cementitious composites aids in enhanced the early and later
122 age properties of cementitious composites [23-24, 26]. Hasty pozzolanic reaction and nano-
123 filler effect of nano-silica improved the microstructure of cement composites and thereby
124 assisted in attaining better resistance to permeability of aggressive ions [27]. It was
125 understood from previous experimental study carried out on PCM based cementitious
126 mortar integrated with nano-silica that drawbacks of PCM based cementitious composites
127 in terms of engineering, hydration and microstructure properties can be tailored by
128 integrating a highly pozzolanic nano-silica particles [6]. But, after reviewing considerable
129 amount of research articles it was observed that no studies have specifically focused on the
130 combined effect of nano silica and PCM in cementitious composites with respect to
131 aggressive ions. Further, lack of investigations on the effects of direct incorporation of bulk
132 PCMs on the same is also noticed. Consequently, there is a need to provide more emphasis
133 on PCMs and PCMs in combination with nano-silica performance against aggressive ions
134 for its better usage in structures at varied climatic region.

135 In this perspective, the present experimental study was carried out to demonstrate the effect
136 of direct incorporation of bulk PCM (n- octadecane) in cementitious mortar on different
137 aggressive exposure conditions such as sulfuric acid (acidic), sodium hydroxide (alkaline)
138 and sodium chloride (chloride). PCM was directly added to cementitious mortar mix at the
139 levels of 1%, 3% and 5% by weight of the binder without replacement to any ingredients.
140 Influence of aggressive ions on compressive strength, density and length changes of PCM
141 added cementitious mortar cured for 28 days at various exposure periods were investigated.
142 Subsequently, PCM based cementitious mixes were modified by integrating optimum
143 dosage of nano-silica (3%) to improve the resistivity towards aforementioned aggressive
144 conditions and the same were studied. Thermogravimetric analysis integrated with
145 differential thermogravimetric (TG-DTG) studies were employed to quantify the formation
146 of deleterious compounds such as ettringite (AFt), gypsum (Gy) and Freidel's salt (Fs) at

147 various temperature ranges of 50-150 °C, 120-150 °C and 230 to 380 °C, respectively.
 148 Further, PCM deterioration due to the same was determined on the basis of
 149 thermogravimetric mass loss at the temperature range of 250 - 300 °C.

150

151 2. Experimental investigation

152 2.1. Materials and material properties

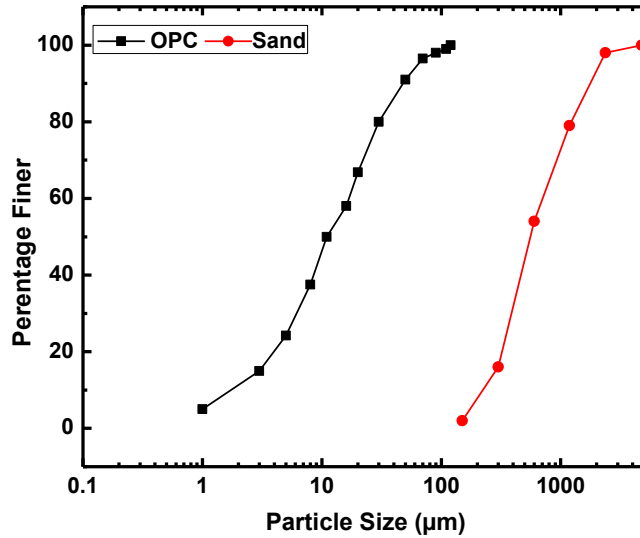
153 Material used in this study for the preparation of cement mortar includes commercially
 154 available ordinary Portland cement (OPC) in compliance to ASTM Type I [28], organic
 155 based PCM i.e. n-octadecane (n-oct, $\text{CH}_3(\text{CH}_2)_{16}\text{CH}_3$), water-based and sodium-stabilized
 156 colloidal nano-silica (CNS, 20 nm) and zone II river sand as fine aggregate (confirming to
 157 IS 383-2016 [29]).

158 Material properties of the ingredients used in present study are given in Table 1 and the
 159 particle size distribution of the materials used are presented in Figure 1.

160 **Table 1.** Physical properties of the cement and fine aggregate used in the study

Material G used	ρ m ² /kg	SC	Setting time (min)		FM	Appearance	MP (°C)	LH (J/g)	Solid Content (w/v)	SiO ₂ content	
			IST	FST							
OPC	3.15	300	32	110	170	-	powder	-	-	-	-
River sand	2.56	-	-	-	-	3.14	grains	-	-	-	-
PCM* (n-oct)	0.78	-	-	-	-	-	oil	26-29	289.4	-	-
CNS*	1.7	2,00,000	-	-	-	-	liquid	-	-	40%	99.5

161 *Manufacturers data, G- Specific Gravity, SC- Standard Consistency, IST-Initial Setting Time, FST-Final Setting
 162 Time, FM-Fineness Modulus, ρ - fineness, MP-melting point, LH-latent heat of fusion.



163

164 **Figure 1.** Particle size distribution curve of the materials used in this study

165 2.2. Mix proportions

166 Total eight mortar mixes were prepared in this study. Among these mixes one is control
 167 mix (with no PCMs and Ns) which was considered to be as reference mix. It is to be noted
 168 that PCM (n-octadecane) is directly added to the mortar mixes without replacing any of the
 169 mortar ingredients at 1%, 3% and 5% by weight of OPC. On the other hand, optimum
 170 dosage of nano-silica (3%) was used as a partial replacement to OPC [6, 23]. For all the
 171 mixes, constant water to binder ratio and water to sand ratio of 0.5 and 1:3 were adopted
 172 in this experimental study. It is to be noted that care was taken on calculating water content
 173 for particular mixes consisting of colloidal nano-silica (i.e. amount of water present in
 174 colloidal nano-silica was adjusted by deducing it from total water content). The detailed
 175 mix proportion along with mix designation for all the mixes are furnished in the Table 2.

176

Table 2. Mix proportions for various mortar mixes used in present study

Mix	Mix Designation	OPC	Ns	PCM	Cement	Ns	PCM	Sand	Water
		%			Quantity (kg/m ³)				
Control	CM	100	-	-	568.35	0	0	1705.1	284.2
OPC + nano-silica - 3%	CNS-3M	97	3	-	551.30	17.05	0	1705.1	258.6
OPC + n-octadecane-1%	oct-1M	100	-	1	568.35	0	5.68	1705.1	284.2
OPC + n-octadecane-3%	oct-3M	100	-	3	568.35	0	17.05	1705.1	284.2
OPC + n-octadecane-5%	oct-5M	100	-	5	568.35	0	28.42	1705.1	284.2
OPC + 3% nano-silica + n-octadecane-1%	CNS/oct-1M	97	3	1	551.30	17.05	5.68	1705.1	258.6
OPC + 3% nano-silica + n-octadecane-3%	CNS/oct-3M	97	3	3	551.30	17.05	17.05	1705.1	258.6
OPC + 3% nano-silica + n-octadecane-5%	CNS/oct-5M	97	3	5	551.30	17.05	28.42	1705.1	258.6

178 2.3. Experimental methodology

179 2.3.1. Sample preparation

180 Initially, n-octadecane PCM (in molten form) and CNS (for mortar mixes containing nano-
181 silica) was added to water and uniformly dispersed by means of continuous stirring. Next,
182 OPC and sand were dry mixed for 120 sec at low speed using 5 liter capacity automatic
183 mortar mixer. Finally, water comprising of PCM/Ns or both are added gently and mixed
184 for 120 sec (30 sec at slow speed + 90 sec at high speed). The fresh mortar samples prepared
185 using automatic mortar mixer were cast in designated moulds of the size **70.6 mm x 70.6**
186 **mm x 70.6 mm** (for measuring density and strength losses associated to different chemical
187 exposures) and **25 mm x 25 mm x 285 mm** (for measuring change in length associated to
188 different chemical exposures). Then, samples were made to store in laboratory condition
189 (Temp: 27 ± 2 °C and RH: 95%) for 24 hrs. After 24 hrs samples were demoulded and
190 subjected to saturated water curing for a period of 28 days.

191 2.3.2. Testing methodology

192 Cubical mortar samples of size 70.6 mm x 70.6 mm x 70.6 mm were used to measure the
193 resistance to aggressive chemicals (acid alkali and chloride) in terms of density loss and

194 strength loss. After the specified period of water curing i.e. 28 days, samples were taken
195 out of the water submerged condition and allowed to attain saturated surface dry condition.
196 Compressive strength of all the mixes cured for 28 days were determined using
197 compressive strength testing machine of 2000 kN capacity at the loading rate of 35
198 N/mm²/min (IS 4031 (part 6)-1988) [30] and that was noted as initial compressive strength
199 value (σ_{initial}) of the respective mix. Next, initial density (ρ_{initial}) of the samples before
200 exposing to any chemical solutions were recorded using weighing balance (precision 0.1
201 g). Subsequently, all the samples were exposed to differed chemical solutions by
202 submerging the samples in an independent containers comprising of 1% sulfuric acid (acid
203 environment, pH 0.3), 5% sodium sulfate (alkali environment, pH 12.0) and 5% sodium
204 chloride (chloride environment, pH 7.0) solutions [19-20, 31]. Samples were kept exposed
205 to solutions for the period of 30, 60, 90, 120 and 180 days. Chemical solutions were
206 sporadically checked for pH and maintained accordingly till the long term exposure period
207 of 180 days. After the accomplishment of specified exposure periods, samples were taken
208 out of the exposure media and allowed to attain surface dry condition. Subsequently,
209 checked for final density (i.e. ρ_{final}) and compressive strength (σ_{final}) at particular period of
210 exposure. Density loss (ρ_{loss}) and strength loss (σ_{loss}) percentage of particular mix exposed
211 to certain type and period of exposure were calculated with respect to initial density and
212 strength values [19]. Average of three cubical samples was considered as density loss and
213 strength loss value for corresponding mix at specified type and duration of exposure.

214 Mortar bars of size 25 mm x 25 mm x 285 mm were cast to measure the change in length
215 of the samples exposed to acid, alkali and chloride solutions. Length comparator apparatus
216 (ASTM C490/490M) [32] was used in this study to measure the associated length change
217 of the samples exposed to various exposure media. Prism samples water cured for 28 days
218 were allowed to attain saturated dry condition and the initial comparator reading was noted.
219 Then, all the samples were made to immerse in different chemical solutions such as 1%
220 sulfuric acid (acid environment, pH 0.3), 5% sodium sulfate (alkali environment, pH 12.0)
221 and 5% sodium chloride (chloride environment, pH 7.0) using independent containers with
222 maintained pH throughout the period of exposure. Change in length were checked and kept
223 recording at the exposure periods of 1, 3, 7, 14, 30, 60, 90, 120 and 180 days. Length
224 change of samples were measured in compliance to ASTM C 157/C157M (acid and saline

225 exposure) [33] and ASTM C 10212/1012M (sulfate exposure) standards [34]. Change in
 226 length in terms of micro strains for mortar samples was calculated as per ASTM C596-18
 227 standards [35].

228 Thermogravimetric analysis was carried out using TG/DTA analyzer (Rigaku-TG/DTA
 229 8122). Crushed and grinded mortar samples passing through 75 micron sieve were used to
 230 characterize the thermal mass loss of the chemically exposed PCM based mortar samples.
 231 Test was carried out at nitrogen purge environment (heating rate: 10 °C/min and purge rate:
 232 20 ml/min), at the temperature range of 50–900 °C. On the basis of obtained TGA results,
 233 deleterious compounds formed due to acid and alkali attack i.e. ettringite
 234 ($\text{Ca}_6\text{Al}_2(\text{SO}_4)_3(\text{OH})_{12}\cdot 26\text{H}_2\text{O}$, AFt) and gypsum ($\text{CaSO}_4\cdot 2\text{H}_2\text{O}$, Gy) were quantified using
 235 the Eqs. 1 and 2, respectively considering the mass loss at particular temperature
 236 boundaries of 50-120 °C and 120-150 °C, respectively [19, 36]. Freidel's salt
 237 ($\text{Ca}_2\text{Al}(\text{OH})_6(\text{Cl}, \text{OH})\cdot 2\text{H}_2\text{O}$, Fs) formed due to chloride exposure was quantified using
 238 the Eq. 3 by considering the mass loss at specific temperature range of 230-380 °C [19,
 239 37].

$$240 \quad \text{AFt (\%)} = m_{\text{AFt}} \cdot \frac{M_{\text{AFt}}}{26M_{\text{H}}} \quad (1)$$

$$241 \quad \text{Gy (\%)} = m_{\text{Gy}} \cdot \frac{M_{\text{Gy}}}{2M_{\text{H}}} \quad (2)$$

$$242 \quad \text{Fs (\%)} = m_{\text{Fs}} \cdot \frac{M_{\text{Fs}}}{6M_{\text{H}}} \quad (3)$$

243 Where, m_{AFt} , m_{Gy} and m_{Fs} describes the percentage mass loss linking to AFt, Gy and 6
 244 molecular layer of water from Fs at the temperature ranges of 50-120 °C, 120-150°C and
 245 230- 380 °C, respectively. M_{AFt} , M_{Gy} , M_{Fs} and M_{H} represents the molecular weight of AFt,
 246 Gy, Fs and H_2O i.e, 786.7 g/mol, 172.17 g/mol, 561.3 g/mol and 18.02 g/mol, respectively.

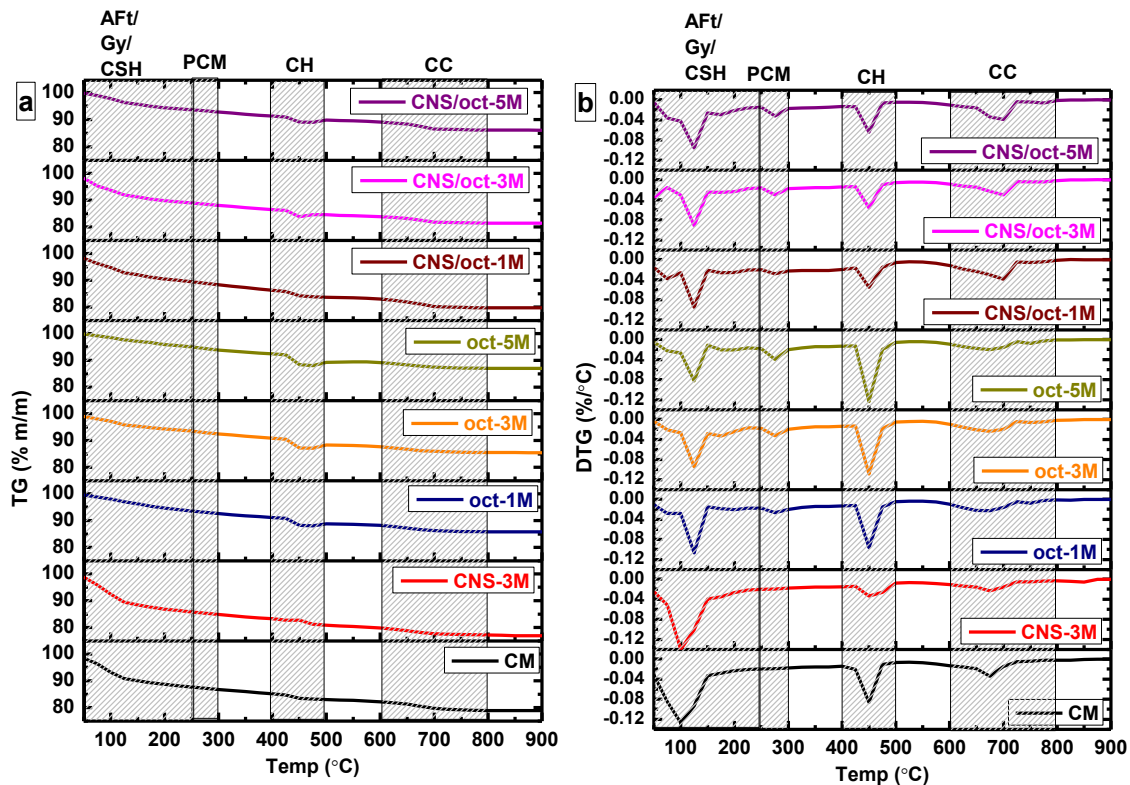
247 Further, percentage of mass loss associated to thermal degradation of PCM based hydration
 248 product (Δm_{PCM}) at the temperature boundaries of 250-300 °C was calculated using Eq. 4.

$$249 \quad \Delta m_{\text{PCM}}(\%) = m_{250^\circ\text{C}} - m_{300^\circ\text{C}} \quad (4)$$

250

251 **3. Results and Discussion**

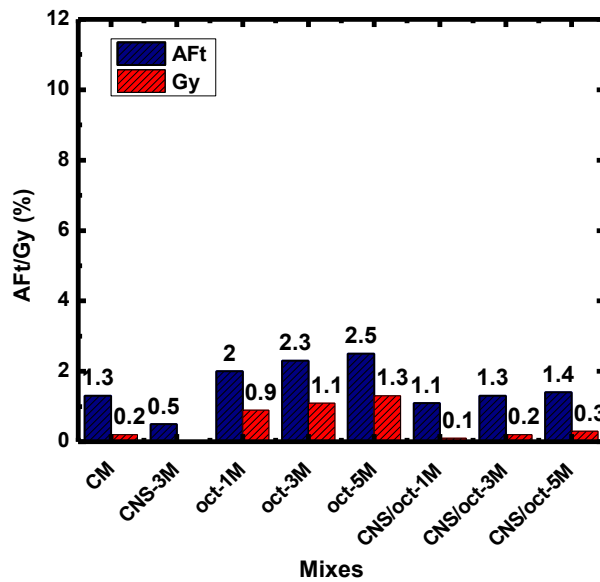
252 **3.1 Thermogravimetric analysis (TG-DTG) - before exposure to aggressive chemicals**



253 **Fig. 2 TG-DTG curve for all the mixes at the curing age of 28 days before exposure to**
 254 **aggressive chemicals**

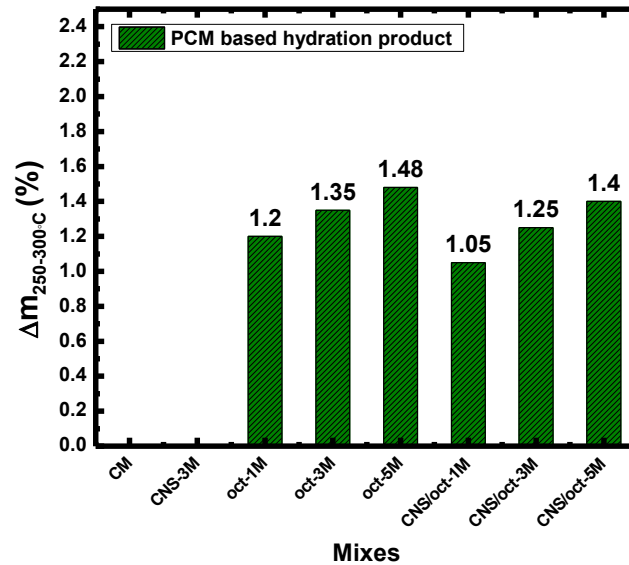
255 Fig. 2 represents the TG-DTG plot for all the cementitious mortar mixes at the curing age of
 256 28 days (without any chemical exposure). Quantification and identification of phases in
 257 cementitious composites are made by considering the mass loss associated to the endothermic
 258 peaks at specific boundaries of temperature i.e., 50-200 °C, 200-300 °C, 400-500 °C and 600-
 259 800 °C. It is reported that formation of phases at the temperature range of 0-200 °C in cement
 260 matrix are complex. Mass loss at 0-50 °C relates to the removal of free molecules of water.
 261 Subsequently, mass losses at 50-120 °C [36], 120-150 °C [36] and 150-300 °C [23] signifies
 262 the decomposition of ettringite (AFt), gypsum (Gy) and dehydration of calcium silicate hydrate
 263 (CSH), respectively. Further, dehydroxylation of calcium hydroxide (CH) and decarbonation
 264 of calcium carbonate (CC) are associated to the mass losses at the particular temperature ranges
 265 of 400-500 °C and 600-800 °C, respectively [6, 23]. It is important to note that all PCM added

266 cementitious composite mixes showed additional endothermic peak (Fig. 2b) at the
 267 temperature range of 250-300 °C indicating the PCM decomposition [5-6]. This study
 268 emphasis on the formation of secondary compounds such as AFt, Gy and Fs due to the action
 269 of aggressive SO_4^{4-} and Cl^- ions. In this regard, amount of AFt and Gy present in all the mixes
 270 at the age of 28 days before exposure to chemical solutions were quantified and presented in
 271 the Fig. 3. There was no endothermic peak relating to the decomposition of Fs (i.e., 230- 380
 272 °C) was observed in case of non-exposed mixes. It is for this reason, plot related to the
 273 quantified amount of Fs is not being presented here.



274
 275 **Fig. 3** Quantified amount of AFt and Gy formed for all the mixes at the curing age of 28 days

276 It can be observed from the Fig.3 that percentage of AFt and Gy formed for all the mixes at
 277 the curing age of 28 days falls below 3%. Amount of AFt and Gy formed for control mix was
 278 found to be 1.3% and 0.2%, respectively. Resulted amount of AFt and Gy for CNS-3M mix
 279 was found to be negligible at the age of 28 days i.e., 0.5% and 0%, respectively. While the
 280 mixes composing of PCM showed higher percentage of AFt and Gy, that found to be increased
 281 by 52%-90% and 50%-90%, respectively in correspondence to control mix. It is important to
 282 note that formation of AFt and Gy was found to be reduced significantly for 3% nano-silica
 283 modified PCM based cementitious mixes with respect to PCM based cementitious mixes
 284 without nano-silica i.e., 50%-60% and 60%-80%, respectively. This is mainly attributed to the
 285 difference in hydration activity exits due to the occurrence of PCMs [5, 6, 9].



286

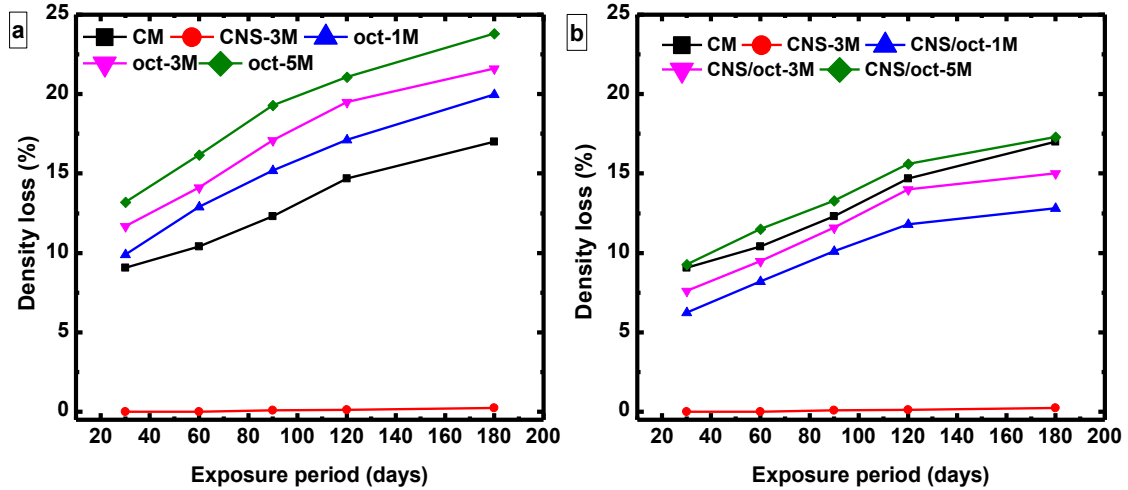
287 **Fig.4** Mass loss percentage related to decomposition of PCM based hydration product at the
 288 curing age of 28 days

289 Mass loss percentage related to decomposition of PCM based hydration product at the curing
 290 age of 28 days is presented in Fig. 4. Mass loss percentage for PCM added cementitious
 291 composites (i.e. oct-mixes) at the temperature boundary of 250-300 °C is found to be in the
 292 range of 1.2% to 1.5%. While, for 3% nano-silica modified PCM based cementitious mixes
 293 (CNS/oct-mixes) it was seen to be reduced by 5%-10%. It is to be noted that PCM based
 294 cementitious mixes both with and without nano-silica showed the existence PCM in
 295 cementitious matrix after the curing age of 28 days. However, it is reported that compressive
 296 strength of cementitious composites drastically reduces due to the crosslinking action of PCM
 297 with hydration product (C-S-H). Further, intrusion of optimum dosage of nano-silica stabilizes
 298 the disturbed PCM based cementitious matrix [6]

299 3.2 Exposure to acid (H₂SO₄) solution

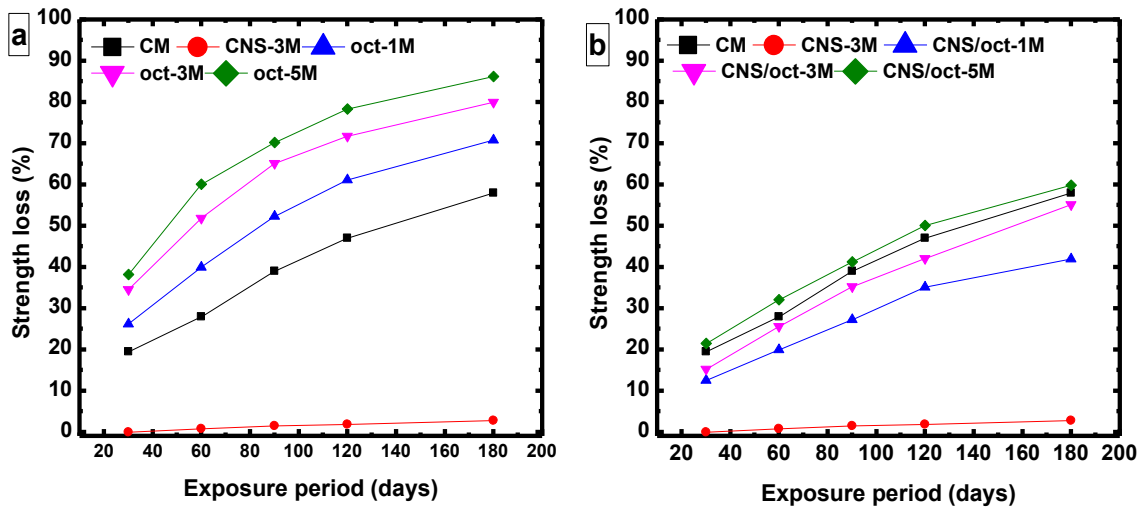
300 3.2.1 Density loss, strength loss and length change

301 Resulted density and strength loss values for PCM added cementitious mortar mixes (with and
 302 without nano-silica) in comparison to control and optimized nano-silica (CNS-3M) mixes
 303 exposed to sulfuric acid solution for the contact periods of 30, 60, 90, 120 and 180 days are
 304 presented in Fig. 5 and Fig. 6, respectively.



305
306
307
308
309

Fig. 5 Percentage of density loss for a) PCM added cementitious composite (oct-mixes)
b) 3% nano-silica modified PCM added cementitious composite (CNS/oct-mixes)
exposed to sulfuric acid (H_2SO_4)



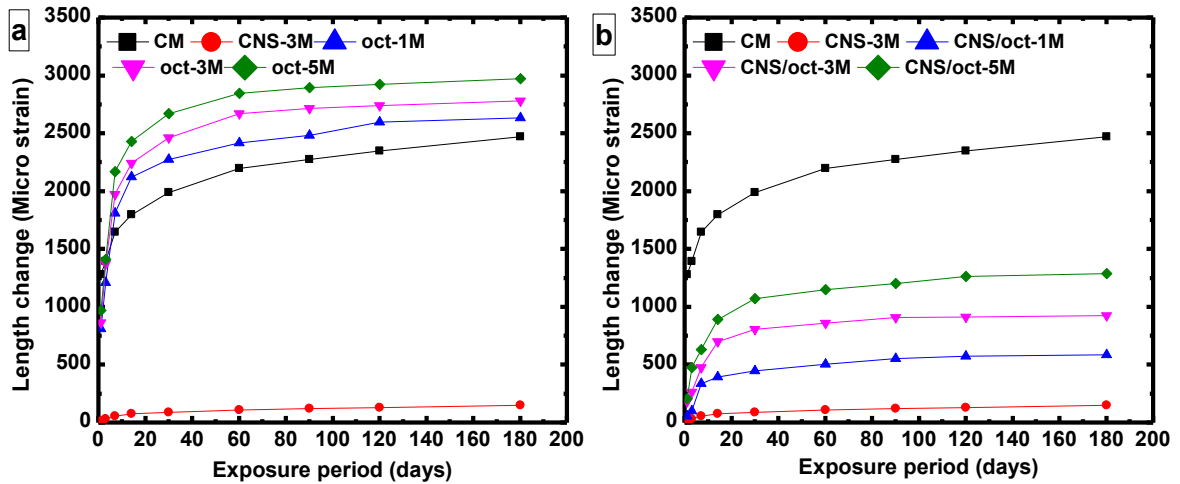
310
311
312
313

Fig. 6 Percentage of strength loss (%) for a) PCM added cementitious composite (oct-mixes)
b) 3% nano-silica modified PCM added cementitious composite (CNS/oct-mixes)
exposed to sulfuric acid (H_2SO_4)

314 It can be observed from Figs. 5 and 6 that among all the mixes CNS-3M mix showed the
315 least deterioration. Percentage of density and strength loss for CNS-3M mix at the exposure
316 period of 180 days was found to be 0.23% and 2.4%, respectively i.e. 98% (density loss)
317 and 96% (strength loss) lower compared to that of control mortar mix. This is ascribed to
318 the high pozzolanic reactivity of nano-silica which aids in reducing initial calcium

319 hydroxide (CH) content. Further, amplified reactivity of nano-silica led to the densification
320 of cementitious matrix **and assists** in controlling the further diffusion of aggressive ions.
321 While, rate of deterioration was observed to be higher for PCM added cementitious mortar
322 (oct-mixes) mixes in proportionate to PCM dosage as compared to that of control mortar.
323 Density and strength loss percentage experienced by 5% PCM added cementitious mortar
324 (oct-5M mix) was 25% and 85%, respectively at the exposure period of 180 days. This is
325 mainly attributed to the deleterious act of sulfuric acid (H_2SO_4) on the weak cementitious
326 matrix comprising of PCM and it is also augmented through the combined act of acid and
327 **sulfate** attack [38]. Exposure to H_2SO_4 would cause dissolution and leaching of acid-
328 susceptible constituents such as calcium hydroxide leading to the formation of gypsum, a
329 soft sulfate di hydrate mineral [39]. Further, this compound along with other sulfate
330 compounds reacts with aluminate phases of cement to form voluminous hydrous calcium
331 aluminium sulfate mineral identified as ettringite [39-40]. It is reported that this action
332 results in an increase in capillary porosity, loss of cohesiveness and eventually losses the
333 strength [38]. It can be understood from the obtained results that by incorporating 3% nano-
334 silica to PCM based cementitious mortar (CNS/oct) which are vulnerable to H_2SO_4 , the
335 rate of deterioration can be minimized. Figs. 5b and 6b also depicts that CNS/oct-1M and
336 CNS/oct-3M exhibits lower percentage of density and strength losses compared to that of
337 control mortar irrespective of exposure period. While, density and strength losses **for**
338 CNS/oct-5M found to be 2% and 3%, higher to control mortar, respectively. Hence, it can
339 be inferred that to reduce the deterioration of the PCM based cementitious matrix occurred
340 due to the intrusion of acid, it is desirable to incorporate highly active pozzolanic ingredient
341 that aids in improving the density and uniformity of the cementitious matrix.

342 Fig. 7 demonstrates the variation in length change for 1%, 3% and 5% PCM based
343 cementitious mortar mixes (with and without nano-silica) in comparison to control and
344 optimized nano-silica (CNS-3M) mixes, when exposed to 1% H_2SO_4 solution for different
345 periods of exposure.



346

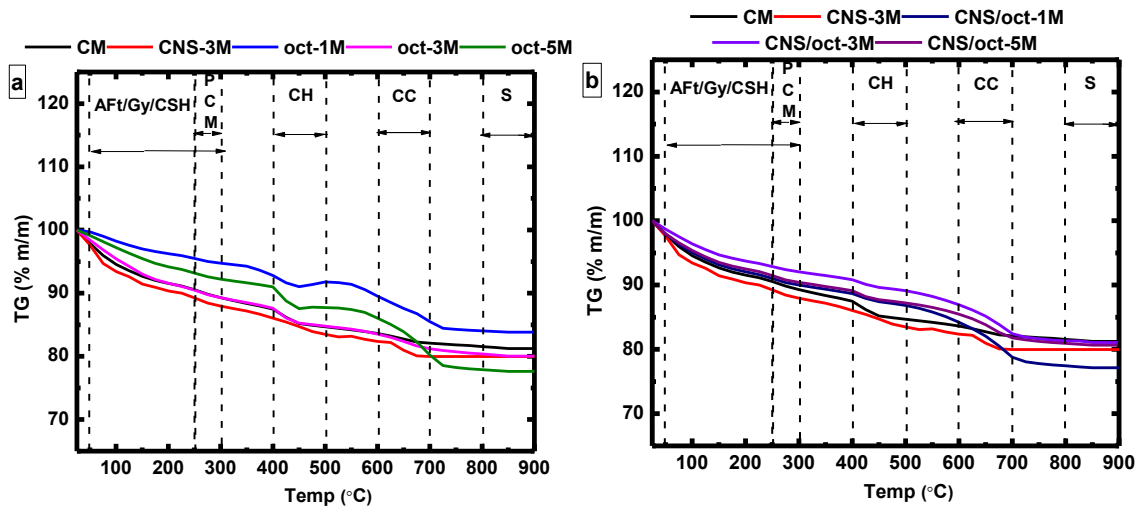
347 **Fig. 7** length change in micro strain for a) PCM added cementitious composite b) 3%
 348 nano-silica modified PCM added cementitious composite exposed to sulfuric acid
 349 (H_2SO_4) solution

350 It can be seen from the Fig. 7 that all mortar specimens with and without PCMs exposed to
 351 H_2SO_4 undergoes expansion over the period of exposure. This expansion is caused due to the
 352 reactivity of **sulfate** ions with calcium aluminates (C_3A) and calcium hydroxide (CH) leading
 353 to the development of expansive compounds such as secondary ettringite (AFt) and secondary
 354 gypsum (Gy) [39-40]. It can be perceived from the **Fig. 7** that control mortar experiences a
 355 length change of approximately 2500 micro strains at the exposure period of 180 days. Results
 356 also shows that CNS-3M mortar mix comprising of 3% nano-silica experiences negligible
 357 change in length as compared to that of control mortar and other PCM based mortar mixes.
 358 Maximum value of length change for CNS-3M was observed to be as 130 micro strain at the
 359 **exposure age** of 180 **days**. This could be ascribed to the reduction in CH content and improved
 360 microstructure of cementitious mortar owing to the high pozzolanic and nano-filling action of
 361 nano-silica particles. It can be perceived from the figure that in case of PCM based
 362 cementitious mortar mixes (oct-mixes) rate of expansion found to be increased with the
 363 increase in PCM dosage and seen to be higher than that of control mix. Length change values
 364 for oct-1M, oct-3M and oct-5M at the maximum exposure age of 180 days were seen to be
 365 2636 micro strain, 2781 micro strain and 2975 micro strain, respectively. This can be attributed
 366 to the existence of higher percentage of calcium hydroxide owing to the addition of PCMs [6].
 367 In addition to that cross linking of PCM with hydration products weakens the microstructure

368 of cementitious matrix thereby making the system susceptible to deleterious ions [9]. Increased
 369 level of CH in PCM based cementitious system increased the amount of Gy and AFt formation
 370 which are highly expansive compounds responsible for voluminous changes in cementitious
 371 composites. It is reported that these compounds are responsible for increase in volume of
 372 cementitious system by about 1.2 and 2.5 times, respectively [41]. It is to be noted from the
 373 figure that PCM based cementitious mortar integrated with 3% nano-silica (i.e. CNS/oct)
 374 experiences a length change in the range of 586 to 1289 micro strain that falls lower to that of
 375 control mortar. It is evident from the results that rate of expansion of PCM based cementitious
 376 mortar corresponding to H₂SO₄ exposure can be controlled by introducing optimized dosage
 377 of highly reactive nano-silica particles which has a potential to imbibe lime, fore most
 378 susceptible compound in the formation of secondary expansive compounds.

379 3.2.2 Thermogravimetric analysis (TG-DTG)

380 In order to understand the influence of H₂SO₄ on PCM added cementitious composites
 381 thermogravimetric analysis (TG-DTG) was carried out. Figs 8 and 9 demonstrate the TG
 382 and DTG plots for 1%, 3% and 5% PCM based cementitious mortar mixes (with and
 383 without nano-silica) in comparison with control and optimized nano-silica (CNS-3M)
 384 mixes, when exposed to 1% H₂SO₄ solution for the period of 180 days.



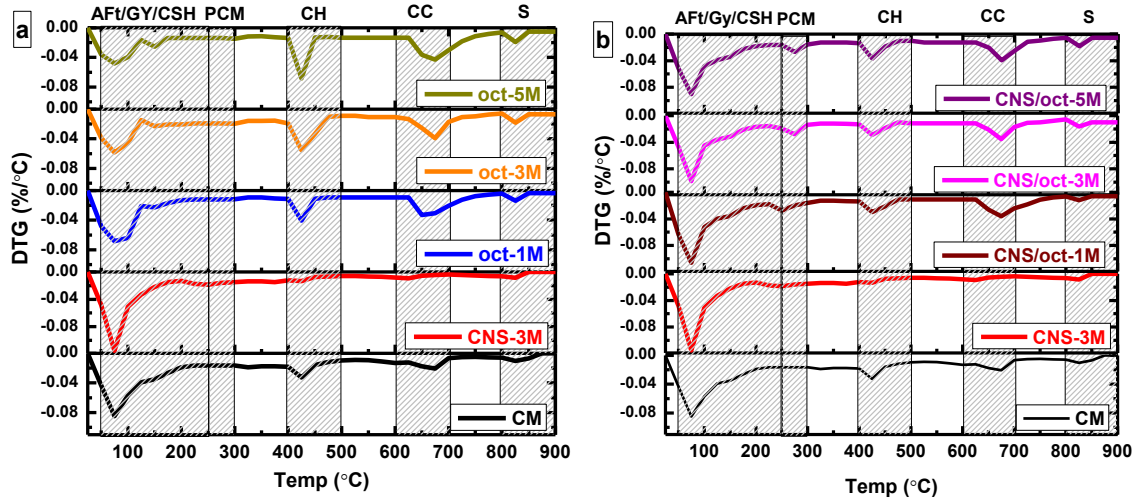
385

386 **Fig. 8** TGA plot of a) PCM added cementitious composite b) 3% nano-silica modified

387

PCM added cementitious composite exposed to sulfuric acid (H₂SO₄)

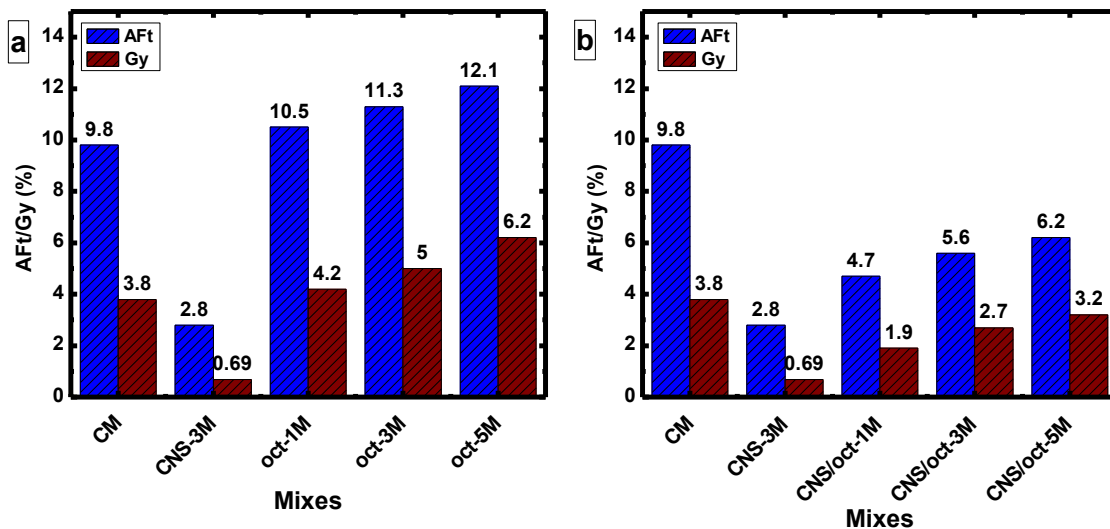
388



389

390 **Fig. 9** DTG plot of a) PCM added cementitious composite b) 3% nano-silica modified
 391 PCM added cementitious composite exposed to sulfuric acid (H_2SO_4)

392 Ettringite (AFt) and gypsum (Gy) are the two major compounds formed due to the
 393 deleterious action of SO_4^{4-} ions, which are responsible to the deterioration of cementitious
 394 composites. On the basis of TG-DTG results amount of AFt and Gy formed for all the
 395 mixes during 180 days of H_2SO_4 exposure were quantified using Eqs 1 and 2 at specific
 396 temperature ranges of 50-120 °C and 120-150 °C, respectively. The same are graphically
 397 presented in Fig. 10.

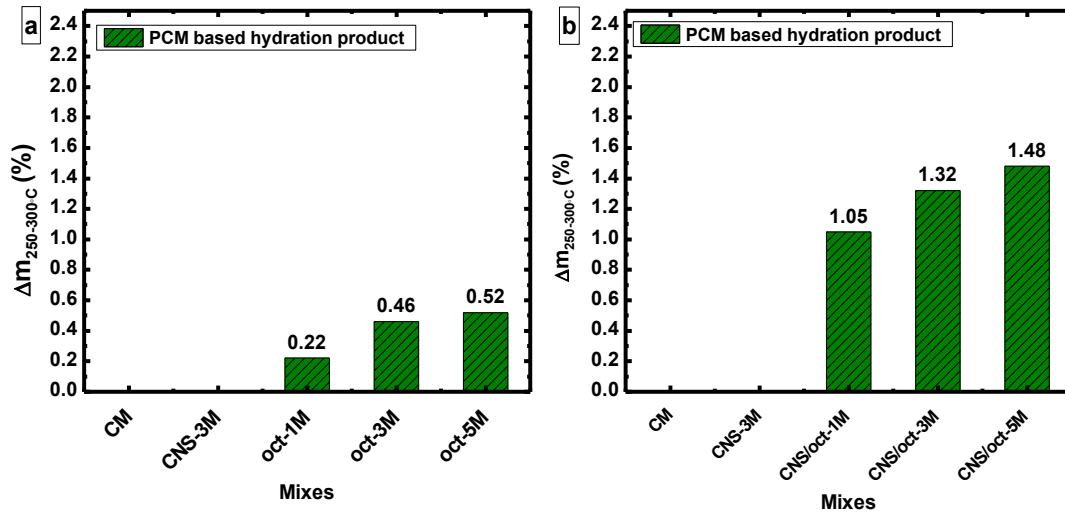


398

399 **Fig. 10** Quantified amounts of AFt and Gy for a) PCM added cementitious composite b)
 400 3% nano-silica modified PCM added cementitious composite exposed to sulfuric acid
 401 (H_2SO_4) solution for 180 days

402 It can be observed from the figure that least formation of AFt and Gy was obtained for
403 CNS-3M mix. This is attributed to the greater consumption of CH by means of high
404 reactivity rate of nano-silica and formation of densified cementitious matrix owing to its
405 physico-chemical activity [42]. It can also be inferred from the figure that AFt and Gy
406 content for oct-mixes found to be increased with the increase in PCM dosage. Further, it is
407 evident from the figure that AFt and Gy content for PCM added cementitious mixes (oct-
408 mixes) found to be increased by 8-24% with respect to that of control mix. This is ascribed
409 to the increase in CH content with increased dosage of PCM in cementitious mixes. This
410 can be substantiated through the increase in endothermic peak height associated to
411 dehydroxylation of CH (at 400-500 °C) with the increase in PCM content (Fig. 2b). It is to
412 be noted from the Fig. 10 that amount of formation of AFt and Gy for PCM based
413 cementitious mixes were found to be modified by the integration of 3% highly reactive
414 nano-silica particles i.e., CNS/oct mixes. Formation rate of AFt and Gy content for
415 CNS/oct mixes were found to be reduced by $\approx 50\%$ with respect to PCM based cementitious
416 mixes (oct-mixes). This is mainly attributed to the progressive action of nano-silica on
417 PCM added cementitious mixes by minimizing the pores generated through the
418 incorporation of PCMs, instigating the pozzolanic reactivity and reducing the
419 concentration of CH with in the PCM based cementitious system [6].

420 In addition, it is important to note from the Fig. 9 that for CNS/PCM mixes there exists an
421 extra endothermic peak at the temperature boundaries of 250-300 °C, which indicates the
422 decomposition of PCM (octadecane) linked calcium silicate hydrate. However,
423 endothermic peak referring to PCM was found to be absent in PCM based cementitious
424 mixes without nano-silica (oct-mixes). This could be attributed to extermination of PCM
425 in cementitious mixes exposed to H₂SO₄. Whereas, presence of nano-silica in PCM based
426 cementitious mixes controlled the deterioration of PCM caused due to H₂SO₄ exposure
427 owing to the refined microstructure of cementitious matrix through the action of nano-
428 silica. This demonstrates that in case of CNS/oct mixes PCMs are still active as a thermal
429 storage material even after the 180 days of H₂SO₄ exposure. In this regard, percentage of
430 mass loss associated to the decomposition of PCM based hydration product (at 250° C-
431 300 °C) was calculated for all PCM added cementitious composites (with and without
432 nano-silica) and the results are presented in Fig 11.



433

434 **Fig. 11** Percentage mass loss of PCM based hydration product at 250° C-300 °C for a)
 435 PCM added cementitious composite b) 3% nano-silica modified PCM added cementitious
 436 composite exposed to sulfuric acid (H₂SO₄) solution for 180 days

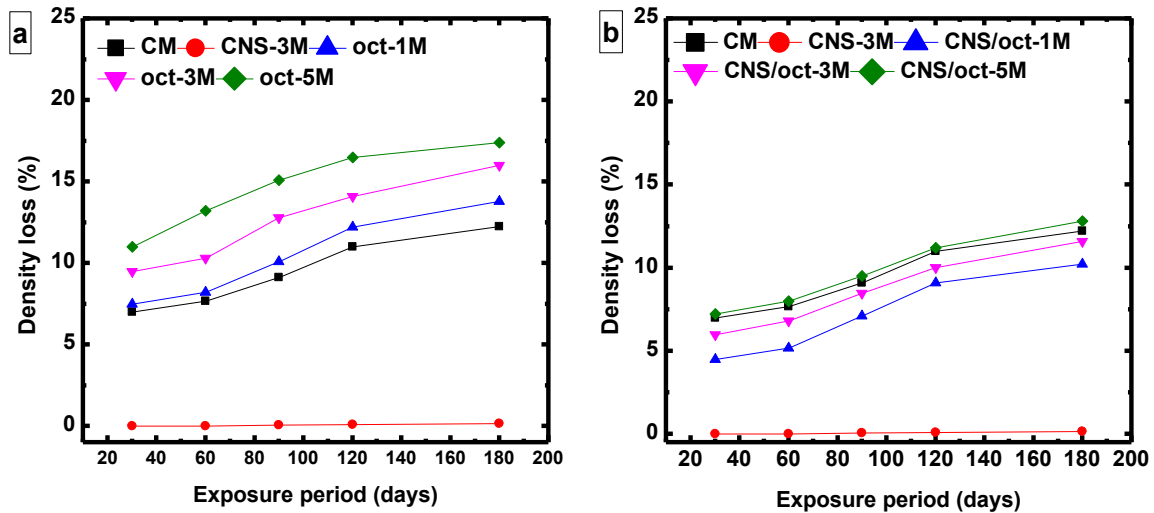
437 It can be seen from the Fig. 11 that percentage of mass loss occurred at 250° C-300 °C for
 438 oct-mixes is lower to that of CNS/oct mixes. However, for oct- mixes mass loss at that
 439 particular temperature relates to the stretching of peaks linking to Aft/Gy/CSH compounds,
 440 there is no additional endothermic peak indicating the existence of PCM traces was noticed
 441 at this particular range of temperature. Whereas, in case of CNS/oct-mixes prominent
 442 endothermic peak was observed at the temperature range of 250° C-300 °C and this
 443 specifies the occurrence of PCM cross-linked C-S-H phase i.e. PCM based hydration
 444 product. It is reported that thermal decomposition of tobermorite phase of C-S-H that
 445 comprises of microstructural crystalline regions with disordered layer structures such as 11
 446 Å/9 Å tobermorite and 11 Å jennite happens at the temperature boundaries of 80° C-300
 447 °C [43]. Here, in case of PCM based mixes owing to the cross linking of PCM with the
 448 tobermorite phase of C-S-H, the associated endothermic found at the temperature range of
 449 250° C-300 °C.

450 3.3 Exposure to alkali (Na₂SO₄) solution

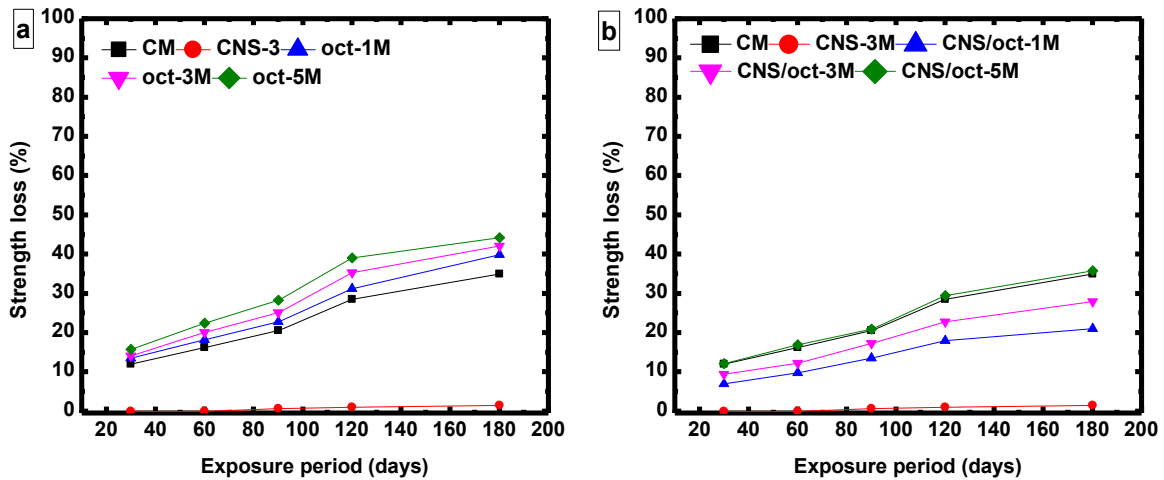
451 3.3.1 Density loss, strength loss and length change

452 Figs. 12 and 13 shows the density loss and strength losses endured by 1%, 3% and 5% PCM
 453 based cementitious mortar mixes (with and without nano-silica) along with control and

454 optimized nano-silica (CNS-3M) mixes, when exposed to 5% Na₂SO₄ solution for the exposure
 455 periods of 30, 60, 90, 120 and 180 days.



456
 457 **Fig. 12** Density loss (%) of a) PCM added cementitious composite b) 3% nano-silica
 458 modified PCM added cementitious composite exposed to sodium sulfate (Na₂SO₄)

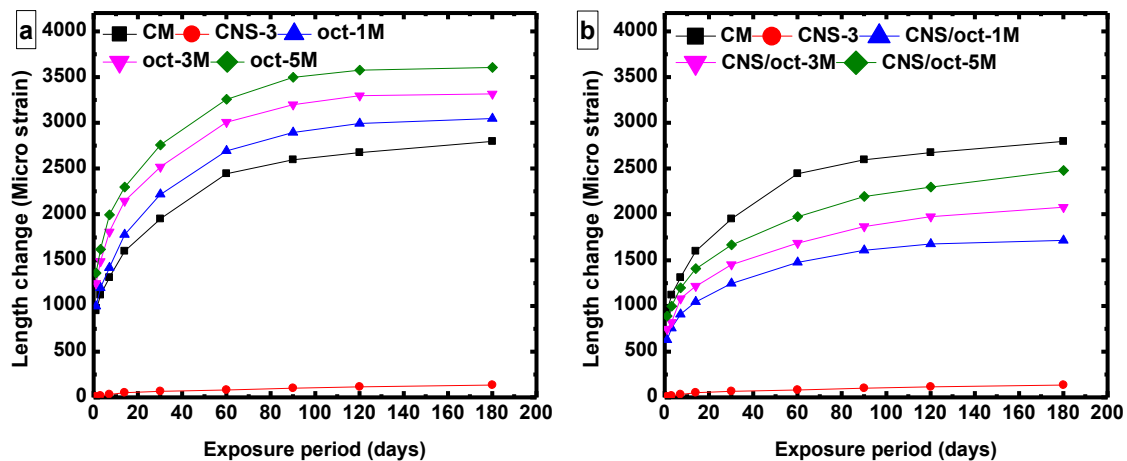


459
 460 **Fig. 13** Strength loss (%) of a) PCM added cementitious composite b) 3% nano-silica
 461 modified PCM added cementitious composite exposed to sodium sulfate (Na₂SO₄)

462 It can be observed from the Figs 12 and 13 that as like H₂SO₄ exposure, CNS-3M mix showed
 463 least deterioration in correspondence to alkali (Na₂SO₄) exposure as well. Density loss and
 464 strength loss values for CNS-3M mix at Na₂SO₄ exposure period of 180 days was found to be
 465 0.16% and 1.5%, respectively. On the other hand, PCM based cementitious mortar mixes (oct-
 466 mixes) experienced greater deterioration as compared to that of control mortar (Fig. 13a).

467 However, alkaline based Na_2SO_4 solution found to be less aggressive compared to that of
 468 acidic H_2SO_4 solution. Among PCM based cementitious mortar mixes, mix comprising of 5%
 469 PCM (oct-5M) suffered highest deterioration with maximum density and strength loss values
 470 of 17% and 44%, respectively at the exposure period of 180 days. Further, it can be understood
 471 from the Fig. 13b that PCM based cementitious mortar mixes when integrated with 3% nano-
 472 silica (CNS/oct- mixes) rate of deterioration caused due to Na_2SO_4 exposure found to be
 473 reduced. Density and strength losses experienced by CNS/oct-1M and CNS/oct-3M were
 474 found to be lower to that of control mortar. It is to be noted that density loss and strength loss
 475 experienced by CNS/oct- mixes were found to be reduced by around 27% and 35%,
 476 respectively with respect to that of oct-mixes at the exposure period of 180 days. This
 477 controlled level of deterioration was due to the presence of nano-silica which compensated the
 478 negative impact of PCMs on the performance of cementitious composites.

479 Length change results of different proportion of PCM added cementitious mixes with and
 480 without nano-silica in comparison to control and 3% nano-silica mix is presented in Fig. 14.

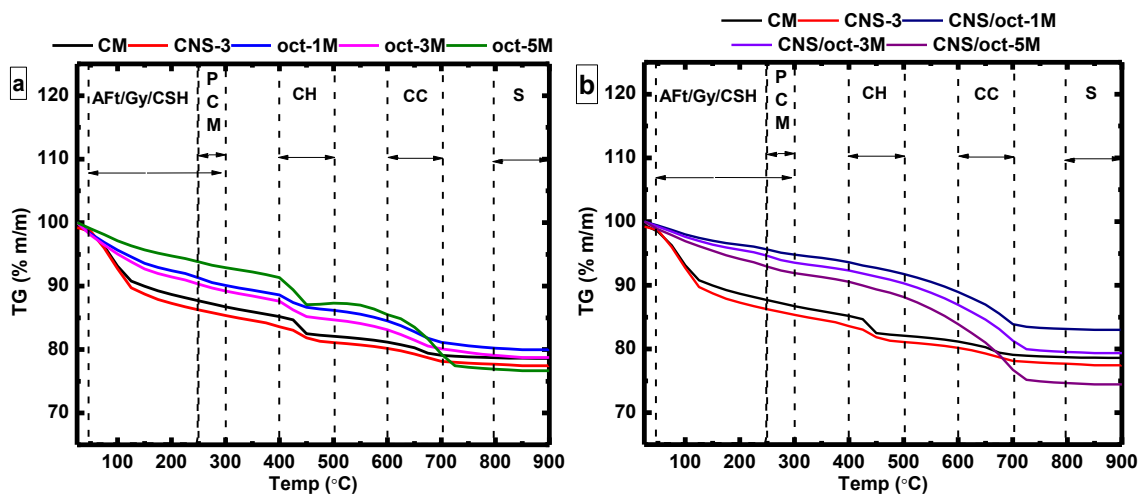


481
 482 **Fig. 14** length change in micro strain for a) PCM added cementitious composite b) 3%
 483 nano-silica modified PCM added cementitious composite exposed to sodium sulfate
 484 (Na_2SO_4) solution

485 From the obtained results it can be noticed that all the mixes tends to expand when exposed
 486 to Na_2SO_4 solution and found to be higher to that of H_2SO_4 exposure. This could be
 487 attributed to the immediate interaction of sulfate ion with the aluminates phases to form
 488 voluminous compounds such as Aft and Gy [44]. It can be noticed from the figure that
 489 expansion rate for CNS-3M mix with 3% nano-silica (as partial replacement to cement)

490 was found to be least i.e. 152 micro strain at 180 days of exposure. High pozzolanic nature
 491 of nano-silica significantly reduced the amount of CH and C₃A content, which are
 492 susceptible for the formation of expansive secondary compounds such as AFt and Gy.
 493 Further, Fig. 14a also illustrates that with increase in **the** addition of PCM content in
 494 cementitious mortar, rate of expansion also found to be increased. PCM added cementitious
 495 mixes (oct-mixes) showed higher expansion than control (2700 micro strain) i.e. in the
 496 range of 3050 to 3610 micro strain. **This could be ascribed to the presence** of PCMs that
 497 disturbed the hydration process by a) cross linking with the hydration products to form
 498 larger traces of calcium hydroxide (Fig. 2), b) diminishing the formation **of C-S-H** and c)
 499 leading to the larger formation of AFt and Gy content. But, the rate of expansion of PCM
 500 based cementitious mixes can be reduced with the addition of 3% nano-silica. Rate of
 501 expansion for CNS/oct- mixes was found to be reduced by 31% - 44% with respect to oct-
 502 mixes. This could be due to the presence of nano-silica which accelerated the pozzolanic
 503 and hydration activity of CNS/oct- mixes thereby resulting in lesser formation of AFt and
 504 Gy.

505 Diffusion of Na₂SO₄ into cementitious matrix also leads in the formation of voluminous
 506 compounds such as AFt and Gy. TG-DTG results of **control, optimized nano-silica and PCM**
 507 **based (with and without nano-silica) cementitious mixes** exposed to 5% Na₂SO₄ solution for
 508 the period of 180 days are presented in Figs. 15 and 16.

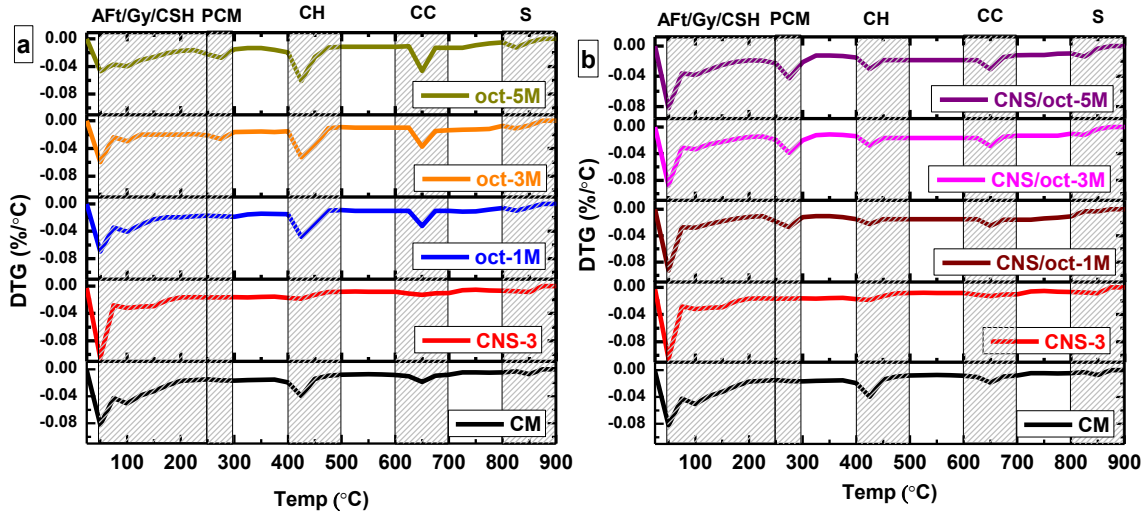


509

510 **Fig. 15** TGA plot of a) PCM added cementitious composite b) 3% nano-silica modified

511

PCM added cementitious composite exposed to sodium sulfate (Na₂SO₄)

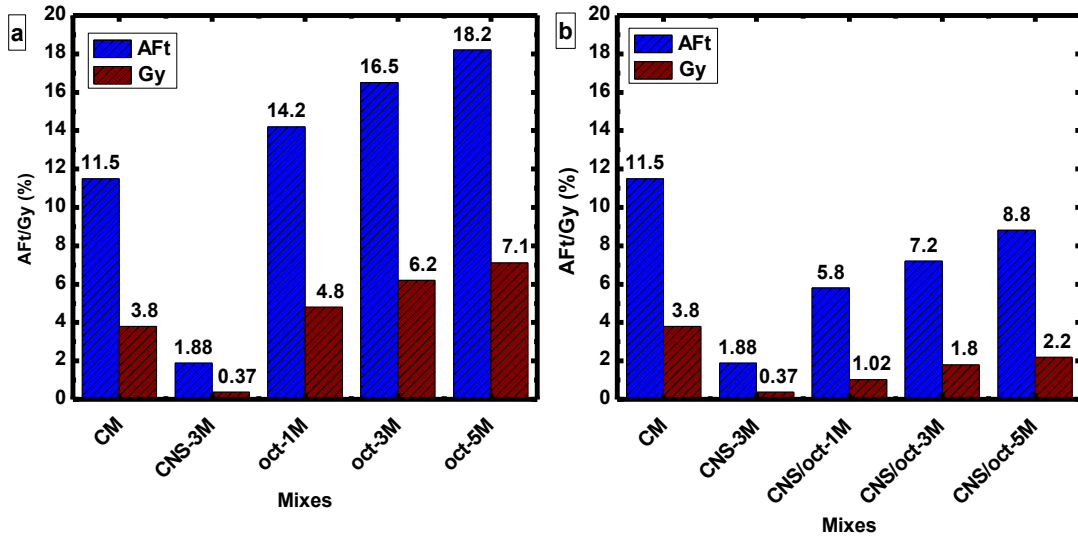


512

513 **Fig. 16** DTG plot of a) PCM added cementitious composite b) 3% nano-silica modified
 514 PCM added cementitious composite exposed to sodium sulfate (Na_2SO_4)

515 It can be observed from the figure that the trend of TG (Fig.15) and DTG (Fig. 16) curves
 516 for Na_2SO_4 exposed PCM based cementitious mixes were found to be similar to H_2SO_4
 517 exposure condition. It is important to note that in case of Na_2SO_4 exposure condition
 518 endothermic peak at the temperature range of 250-300 °C which signifies the PCM
 519 decomposition was also seen to be exist in oct-3M and oct-5M mixes without nano-silica.
 520 This indicates the occurrence of PCM in alkali exposed cementitious mixes at 3-5% PCM
 521 dosages. Further, AFt and Gy formed during Na_2SO_4 exposure of PCM based cementitious
 522 mixes leads to the deterioration of cementitious system.

523 Quantified amount of AFt and Gy for control, 3% nano-silica, PCM (n-octadecane) and
 524 nano-silica modified PCM added mortar mixes exposed to Na_2SO_4 solution for 180 days
 525 are plotted in the form of histogram and presented in Fig. 17 (a-b).

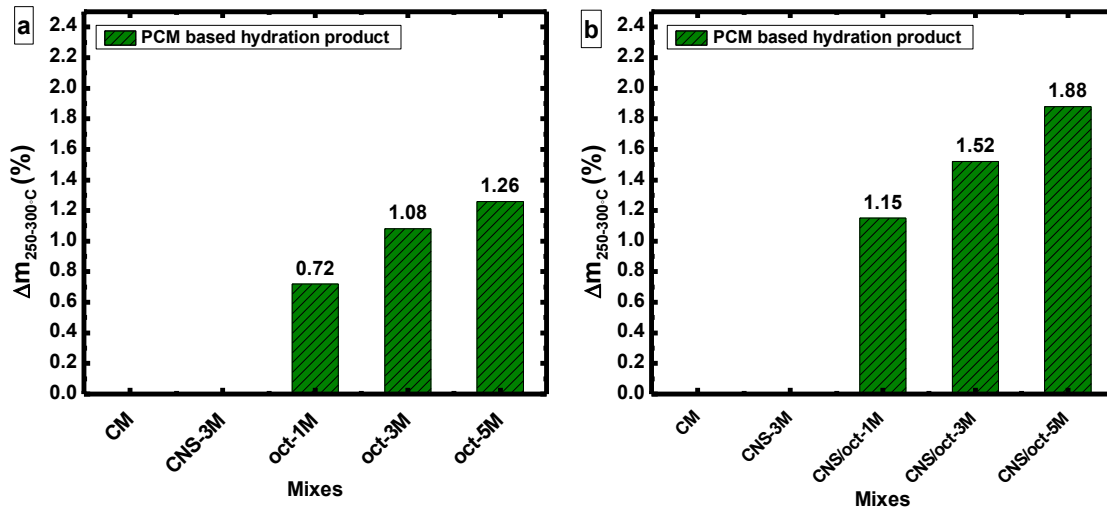


526

527 **Fig. 17** Quantified amounts of AFt and Gy for a) PCM added cementitious composite b)
 528 3% nano-silica modified PCM added cementitious composite exposed to sodium sulfate
 529 (Na_2SO_4) solution for 180 days

530 It can be seen from the Fig. 17 that CNS-3M mix with 3% nano-silica tremendously reduced
 531 the formation of voluminous compounds such as AFt and Gy. This can be attributed to the
 532 existence of negligible traces of CH that can be evinced from the mass loss curve associated
 533 to dehydroxylation of CH (Figs 15 and 16). On the other end, the rate of formation of AFt and
 534 Gy for Na_2SO_4 exposure condition was higher for PCM based cementitious mixes and found
 535 to be increased with the increase in percentage of PCM. AFt and Gy content for oct-mixes
 536 were found to be increased by 23 - 58% and 26 - 87%, respectively with respect to that of
 537 control mix at the exposure age of 180 days. This is attributed to the increase in free lime (CH)
 538 and larger availability of un-hydrated aluminate compounds such as C_3A and C_4AF in
 539 cementitious matrix owing to the presence of PCM and 100% OPC as a binder. It is reported
 540 that PCMs are responsible for increase in capillary porosity in cementitious paste owing to its
 541 negative impact on binding, as it gets adsorbed over the surface of cement grains and hydrated
 542 compounds [5, 9]. Further, it can be noticed from the Fig.17 that for CNS/oct- mixes formation
 543 of AFt and Gy were seen to be curtailed in correspondence to oct-mixes. Amount of AFt and
 544 Gy formed for CNS/oct- mixes were found to be reduced by 51 -60% and 69 -79%, respectively
 545 in correspondence to PCM based cementitious mixes without nano-silica (oct-mixes). This
 546 could be due to the occurrence of highly reactive nano-silica that yields to the reduction of CH

547 concentration and also complemented in minimizing the capillary pores generated through
 548 PCM as well as by CH.



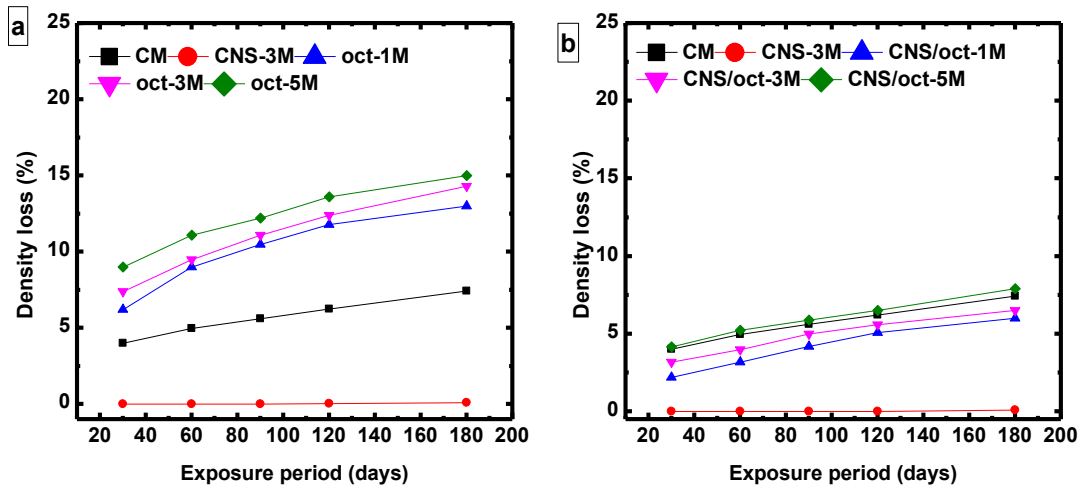
549
 550 **Fig. 18** Percentage mass loss of PCM based hydration product at 250° C-300 °C for a)
 551 PCM added cementitious composite b) 3% nano-silica modified PCM added cementitious
 552 composite exposed to sodium sulfate (Na₂SO₄) solution for 180 days

553 Fig. 18 demonstrates the calculated percentage of mass loss linking to the decomposition
 554 of PCM based hydration product for the mixes exposed to 5% Na₂SO₄ solution for 180
 555 days. It can be noticed from Fig. 18 that the trend of variation in histogram of PCM based
 556 hydration product for Na₂SO₄ exposure found to be in similar to that of H₂SO₄ exposure.
 557 In contrast, in case of Na₂SO₄ exposure there could notice a signature of **endothermic**
 558 peak in the specific temperature range of 250 - 300 °C for oct-3M and oct-5M mixes. This
 559 signposts that percentage of mass loss for oct- mixes related to the PCM cross-linked
 560 hydration product. Further, it is to be noted that percentage of mass loss associated to PCM
 561 based hydration product seen to be increased for CNS/oct-mixes and that found to be
 562 highest for CNS/oct-5 M mix (1.89%). It is reported that tobermorite phase of **C-S-H**
 563 decomposes at the temperature range of 80-300 °C and the results indicate that n-
 564 octadecane based PCM gets adsorbed over the tobermorite phase of **C-S-H** (PCM based
 565 hydrated product), therefore endothermic peak shifts towards the right i.e. at 250-300 °C
 566 [43]. Further, it is understood that this particular phase of **C-S-H** remains stable.

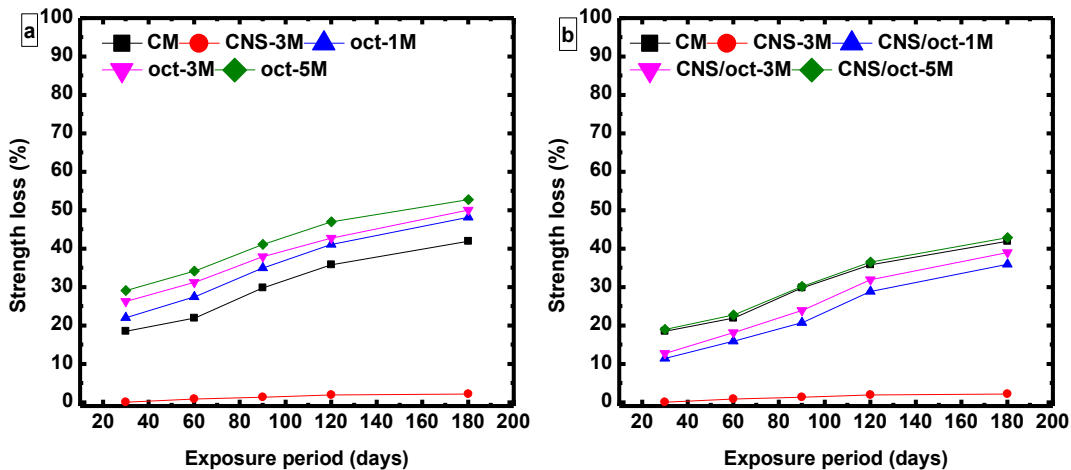
567 3.3 Exposure to chloride (NaCl) solution

568 3.3.1 Density loss, strength loss and length change

569 Figs 19 and 20 presents the density loss and strength loss values for 1%, 3% and 5% PCM
 570 based cementitious mortar mixes (with and without nano-silica) along with control and
 571 optimized nano-silica (CNS-3M) mixes, when exposed to 5% sodium chloride (NaCl) solution
 572 for the duration of 30, 60, 90, 120 and 180 days.

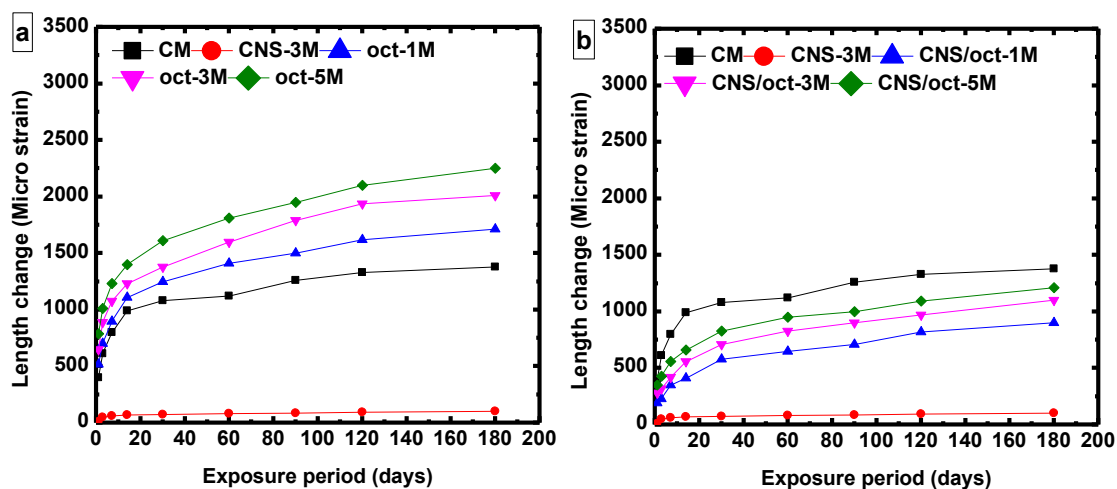


573
 574 **Fig. 19** Density loss (%) of a) PCM added cementitious composite b) 3% nano-silica
 575 modified PCM added cementitious composite exposed to sodium chloride (NaCl)
 576



577
 578 **Fig. 20** Strength loss (%) of a) PCM added cementitious composite b) 3% nano-silica
 579 modified PCM added cementitious composite exposed to sodium chloride (Na₂SO₄)
 580 It can be observed from the figure that as like acid and alkali exposure, CNS-3M mix
 581 showed the least rate of deterioration. It is understood that nano-silica has a greater role in
 582 resisting the action of chloride ions on cementitious system owing to its enhanced physical

583 and chemical activity. In contrast, PCM added cementitious mortars (oct-mixes) showed
 584 highest rate of deterioration at 5% NaCl exposure. Density and strength losses suffered by
 585 oct-mixes were found to be increased by 75-90% and 20-30%, respectively with respect to
 586 control mix at 180 days of exposure. This could be ascribed to the deleterious facts such as
 587 decalcification, leaching of calcium chloride and formation of porous C-S-H [45]. Further,
 588 integration of optimized nano-silica content (i.e. 3%) into the chloride susceptible PCM
 589 added cementitious mortar (CNS/oct- mixes) altered the rate of deterioration. Density and
 590 strength losses experienced by CNS/oct- mixes were found to be reduced by 47-55% and
 591 26-30%, respectively in correspondence to oct-mixes without nano-silica. **This can be**
 592 **attributed to the reduced rate of diffusion of chloride ions** into the cementitious system
 593 owing to the modified microstructure of PCM added cementitious mortar in the presence
 594 of highly reactive nano-silica.
 595 Change in length associated to the NaCl exposure for PCM added cementitious mortar
 596 mixes and nano-silica modified PCM added cementitious mortar mixes in comparison to
 597 control and 3% nano-silica mixes are presented in Fig. 21.



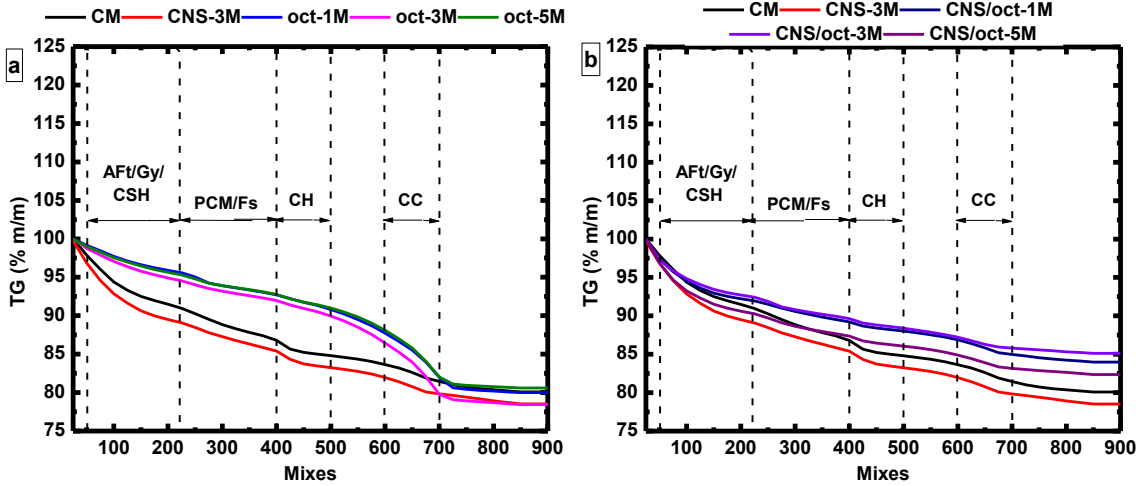
598
 599 **Fig. 21** length change in micro strain for a) PCM added cementitious composite b) 3%
 600 nano-silica modified PCM added cementitious composite exposed to sodium chloride
 601 (NaCl) solution

602 It can be observed from the figure that the trend in variation of length change for control, CNS-
 603 3M and all PCM added cementitious mortar (with and without nano-silica) specimens exposed
 604 to 5% NaCl solution was found to be similar to acid and alkali exposure. CNS-3M mix

605 comprising of 3% nano-silica showed greater resistance to chloride exposure. Expansion value
606 of CNS-3M mix at the exposure age of 180 days was seen to be less than 100 micro strain.
607 This can be attributed to the least formation of Fs owing to the increased consumption rate of
608 unhydrated/hydrated aluminates phases in the cementitious system and filler property of nano-
609 silica, which resisted the diffusion of chloride ions responsible for the formation of Fs [19].
610 PCM added cementitious mortar mixes (oct-mixes) showed highest rate of expansion.
611 Expansion value for oct-mixes at the exposure age of 180 days was found to be in the range of
612 1750-2250 micro strain which is greater to that of control mix (1300 micro strain). This is
613 mainly attributed to the increased porosity owing to the excessive formation of CH and
614 disturbed hydration system in cementitious composite [6]. Further, leading to the enhanced
615 ingress of chloride ions into the system, thereby develops expansive stress through the
616 voluminous nature of Fs formed within the hardened cementitious system. It is important to
617 note that incorporation of nano-silica in PCM added cementitious mixes controlled the rate of
618 expansion caused due to NaCl solution. Expansion value for CNS/oct-mixes at the age of 180
619 days falls in the range of 750-1150 micro strain. PCM based cementitious mortar in the
620 presence of nano-silica exhibited better-quality microstructure by tailoring the interruption
621 caused by PCM.

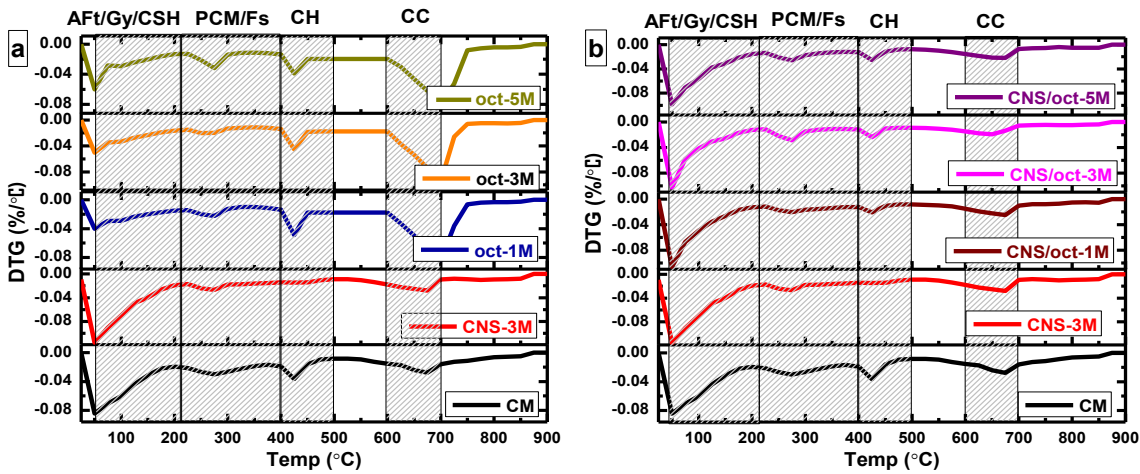
622 Interaction of NaCl with un-hydrated and hydrated phases of aluminates of cementitious
623 system leads to the formation of Friedel's salt (Fs) and its analogues.

624 To analyze the action of NaCl on PCM added cementitious samples thermogravimetric
625 analysis (TG-DTG) was carried out for the samples exposed to the duration of 180 days.
626 TG and DTG plot for the same are presented in Figs. 22 and 23, respectively.



627

628 **Fig. 22** TGA plot of a) PCM added cementitious composite b) 3% nano-silica modified
 629 PCM added cementitious composite exposed to sodium chloride (NaCl)

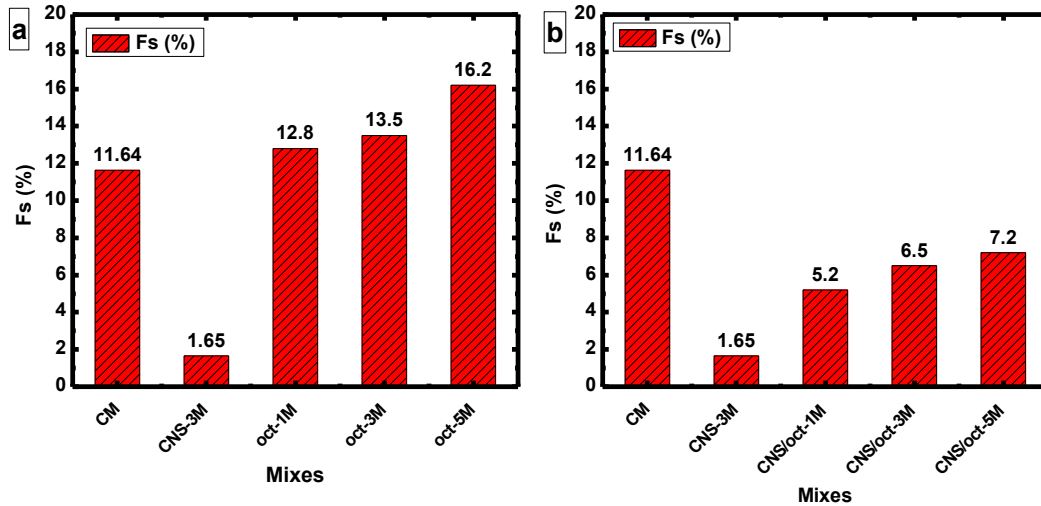


630

631 **Fig. 23** DTG plot of a) PCM added cementitious composite b) 3% nano-silica modified
 632 PCM added cementitious composite exposed to sodium chloride (NaCl)

633 It can be observed from the Figs. 22 and 23 that 180 days NaCl exposed PCM based mortar
 634 mixes (with and without nano-silica) also undergoes series of thermogravimetric mass
 635 losses at various temperature ranges similar to acid (H_2SO_4) and alkali (Na_2SO_4) exposed
 636 mixes. It can be noticed from the Fig. 23 that in case of NaCl exposed mixes, there exists
 637 endothermic peak for all the mixes at the temperature range of 230-400 °C which indicates
 638 the overlapping of endothermic peaks developed through the decomposition of two
 639 compounds i.e. Friedel's salt (Fs, 230-380 °C) and PCM (250-300 °C). Accordingly,
 640 endothermic peak in this particular range of temperature is observed to be broadened.

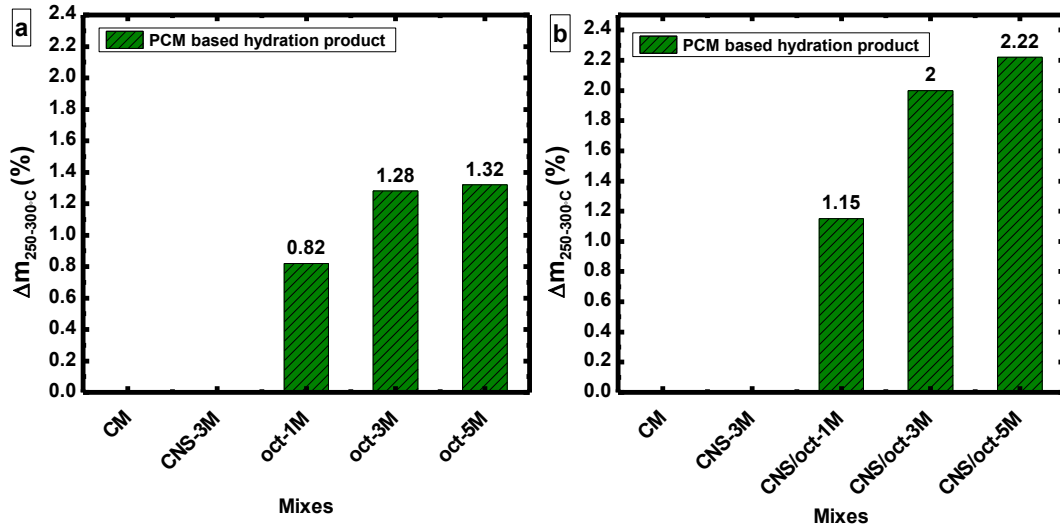
641 Quantified amount of chemically bound Fs content for control, nano-silica, PCM (n-
 642 octadecane) and nano-silica/PCM based mortar mixes exposed to 5% NaCl solution is
 643 shown in Fig. 24.



644

645 **Fig. 24** Quantified amounts of Fs for a) PCM added cementitious composite b) 3% nano-
 646 silica modified PCM added cementitious composite exposed to sodium chloride (NaCl)
 647 solution for 180 days

648 Fig. 24 demonstrates the significant drop in Fs content for CNS-3M mix i.e. 86% lower to that
 649 of control mix. This could be attributed to the following actions of nano-silica: a) consuming
 650 the CH, b) supplementary formation of dense C-S-H, c) nano filler effect and d) reduced
 651 concentration of chloride vulnerable compounds such as C_3A and C_4AF . At the same time,
 652 amount of Fs formed for PCM added cementitious mixes (oct-mixes) were found to be
 653 increased by 10-40% with respect to that of control mix and are directly proportional to the
 654 percentage of PCM added. This could be attributed to the occurrence of higher concentration
 655 of portlandite (CH) and aluminate phases (C_3A , C_4AF and AFm) [5, 9, 46]. Further, in case of
 656 nano-silica modified PCM added cementitious mixes (CNS/oct- mixes) despite of the
 657 disruption in hydration process caused by PCM, presence of highly reactive nano-silica scaled
 658 down the formation of Fs. Amount of Fs formed in CNS/oct mixes were found to be reduced
 659 by 47-50% and 52-55% in correspondence to control and PCM based cementitious mixes (oct-
 660 mixes), respectively. This indicates that resistance to chloride ion for PCM added cementitious
 661 mixes can be enhanced by integrating 3% of nano-silica.



662

663 **Fig. 25** Percentage mass loss of PCM based hydration product at 250° C-300 °C for a)
 664 PCM added cementitious composite b) 3% nano-silica modified PCM added cementitious
 665 composite exposed to sodium chloride (NaCl) solution for 180 days

666 Percentage of mass loss derived from TG-DTG analysis for decomposition of PCM at
 667 temperature boundaries of 250 to 300 °C is plotted in Fig. 25. It can be noticed from Fig.
 668 23 that all the mixes displays the endothermic peak at this range of temperature indicating
 669 the decomposition of hydration product linking to PCM. It can be inferred from Fig. 25
 670 that PCM added cementitious mixes containing 3% nano-silica (CNS/oct- mixes) exhibits
 671 greater Percentage of mass loss associated to decomposition of PCM based hydration
 672 product and it is found to be 50-68% higher to that of oct-mixes. This is ascribed to
 673 presence of PCM in cementitious system are responsible for the increase in the permeable
 674 porosity of cementitious composites owing its interruptive nature and incompatibility with
 675 that of hydrated cementitious system [5, 19]. This leads to the increase in diffusion of
 676 chloride ions into the transpired pores and acts as a barrier to the function of PCM, further
 677 aggressive chloride media causes deterioration of PCM. Nano-silica being a loftier material
 678 aids to the significant reduction in porosity, simultaneously adds to the development of
 679 dense CSH in the cementitious system due to its nucleation mechanism [23] that attributes
 680 to the protection of PCM incorporated cementitious composite from aggressive ions.
 681 Further, it is clear from the obtained results that incorporation of nano-silica does not
 682 weakens the thermal performance of integrated PCM in cementitious system. Due to this
 683 action, strategy of incorporating nano-silica into PCM added cementitious system found to

684 be promising in tackling the influence of aggressivity with retaining the thermal ability.
685 However, it is important to note that in case of chloride exposed mixes there found a
686 discrepancy in the calculated mass loss percentage for PCM based hydration product, since
687 there subsists superimposition of endothermic peak (Fig. 23) responsible for the
688 decomposition of compounds such as Fs and PCM linked **C-S-H phase** (tobermorite like)
689 in the range of 200-400 °C.

690 **4. Conclusion**

691 In this paper, change in phase compositions (AFt, Gy, Fs, PCM based hydration products)
692 happened before and after the action of aggressive solution such as 1% sulfuric acid, 5%
693 sodium hydroxide and 5% sodium chloride were quantified using TG/DTG technique. The
694 effect of PCM (n-octadecane) in the presence and absence of nano-silica (optimal content
695 3%) on aggressive exposure solutions for all the mixes were investigated.

696 All PCM based cementitious mixes (with and without nano-silica) used in this study
697 showed an endothermic peak at 250-300°C relating to the decomposition of PCM cross
698 linked hydration product at the curing age of 28 days and that indicates both the series of
699 PCM mixes are thermally effective. At the same time endothermic peak height at 400-
700 500°C associated to dehydroxylation of portlandite phase increased with the increase in
701 PCM dosage, nevertheless endothermic peak height reduced with the incorporation of
702 highly pozzolanic nano-silica particles.

703 PCM added cementitious mixes experiences extensive loss in density, compressive
704 strength and volumetric stability when exposed to SO_4^{2-} and **Cl⁻** ions. **In contrary**, 3% nano-
705 silica modified PCM added **cementitious** mixes minimized the vulnerability to aggressive
706 ions **and resistivity found to be more compared to that of control mix especially at 1% and**
707 **3% PCM dosages**. Sulfuric acid attack on the weak cementitious matrix in the presence of
708 PCM is more deleterious due to the combined act of acid and **sulfate**. Formation of
709 voluminous secondary ettringite (AFt) and gypsum (Gy) when exposed to SO_4^{2-} ions (at
710 both acid and alkali media) and Friedel's salt (Fs) when exposed to Cl^- ions (at Chloride
711 media) greatly increased for PCM added cementitious mixes (oct-mixes) and 50%
712 reduction is seen in **the PCM based cementitious mix comprising of nano-silica**.

713 It is important to note that after exposing to aggressive solutions (SO_4^{2-} ions and Cl^- ions)
714 endothermic peak occurred at 250° C-300 °C for PCM mixes disappeared. However, for
715 PCM mixes modified with 3% nano-silica, prominent peak was observed at 250° C-300 °C
716 that specifies the occurrence of thermally active PCM. PCMs at this phase cross linked
717 with tobermorite like C-S-H with disordered layer structures such as 11 Å/9 Å tobermorite
718 and 11 Å jennite, and the peak shifts from 80° C-300 °C to 250° C-300 °C.

719 At this point of time it is well understood from the study that there is an essential need to
720 amalgamate highly reactive pozzolanic material like nano-silica to PCM added
721 cementitious mixes in order to have better thermo-mechanical and durability performance.

722

723 **References**

- 724 [1] M. De Gastines, E. Correa, A. Pattini, Heat transfer through window frames in
725 energyplus: model evaluation and improvement. *Adv. Build. Energy Res.* 13 (2019)
726 138–155.
- 727 [2] M. Balbis-Morejón, J. J. Cabello-Eras, J. M. Rey-Hernández, F. J. Rey-Martínez,
728 Energy evaluation and energy savings analysis with the 2 selection of ac systems in an
729 educational building. *Sustainability.* 13 (2021) 7527.
- 730 [3] I. Sarbu, C. Sebarchievici, A comprehensive review of thermal energy storage,
731 *Sustainability.* 10 (2018) 191.
- 732 [4] W. Aftab, A. Usman, J. Shi, K. Yuan, M. Qin, R. Zou, Phase change material-
733 integrated latent heat storage systems for sustainable energy solutions, *Energy Environ.*
734 *Sci.* 14 (2021) 4268-4291.
- 735 [5] K. Snehal, B. B. Das, Effect of phase-change materials on the hydration and mineralogy
736 of cement mortar, *Proc. Inst. Civ. Eng.: Constr. Mater.* (2020) 1-11.
- 737 [6] K. Snehal, B. B Das, S. Kumar, Influence of integration of phase change materials on
738 hydration and microstructure properties of nano-silica admixed cementitious mortar, *J.*
739 *Mater. Civ. Eng.* 32 (6) (2020) 04020108.
- 740 [7] M. Frigione, M. Lettieri, A. Sarcinella, Phase change materials for energy efficiency in
741 buildings and their use in mortars, *Materials (Basel).* 12(8) (2019) 1260.

- 742 [8] M. Gandhi, A. Kumar, R. Elangovan, C. S. Meena, K. S. Kulkarni, A. Kumar, G.
743 Bhanot, N. R. Kapoor, A Review on shape-stabilized phase change materials for latent
744 energy storage in buildings, *Sustainability*. 12(22) (2020) 9481.
- 745 [9] B. Sharma, *Incorporation of phase change materials into cementitious systems*, Thesis,
746 *Arizona state university, USA, 2013*.
- 747 [10] S. Drissi, T. C. Ling, K. H. Mo, A. Eddhahak, A review of microencapsulated and
748 composite phase change materials: Alteration of strength and thermal properties of
749 cement-based materials, *Renew. Sust. Energ. Rev.* 110 (2019) 467-484.
- 750 [11] B. Šavija, Smart crack control in concrete through use of phase change materials
751 (pcms): a review, *Materials*. 11 (2018) 654
- 752 [12] A. Matthew, D. Sumanta, C. Cesar, K. Nihat, S. Gaurav, N. Narayanan, Porous
753 inclusions as hosts for phase change materials in cementitious composites:
754 Characterization, thermal performance, and analytical models, *Constr. Build. Mater.*
755 134 (2017) 574 - 584.
- 756 [13] W. C Choi, B. S. Khil, Y. S. Chae, Q. B. Liang, H. D. Yun, Feasibility of using phase
757 change materials to control the heat of hydration in massive concrete structures, *Sci.*
758 *World J.* (2014).
- 759 [14] S. Ramakrishnan, *Enhancement of thermal performance of buildings using*
760 *cementitious composites containing phase change material*, Thesis, Swinburne
761 *University of Technology Melbourne, Australia, 2017*.
- 762 [15] V. D. Cao, S. Pilehvar, C. S. Bringas, A. M. Szczotok, J. F. Rodriguez, M. Carmona,
763 N. Al-Manasir, A. L. Kjoniksen, Microencapsulated phase change materials for
764 enhancing the thermal performance of Portland cement concrete and geopolymer
765 concrete for passive building applications, *Energy Convers. Manag.* 133 (2017) 56–66.
- 766 [16] M. Hunger, A. G. Entrop, I. Mandilaras, H. J. H. Brouwers, M. Founti, M. The
767 behavior of self-compacting concrete containing micro-encapsulated Phase Change
768 Materials, *Cem. Concr. Compos.* 31 (2009) 731–743.
- 769 [17] A. R. Sakulich, D. Bentz, Incorporation of phase change materials in cementitious
770 systems via fine lightweight aggregate, *Constr. Build. Mater.* 35 (2012) 483–490.
- 771 [18] Z. Zhang, G. Shi, S. Wang, X. Fang, X. Liu. Thermal energy storage cement mortar
772 containing n-octadecane/expanded graphite composite phase change material, *Renew.*
773 *Energy*. 50 (2013) 670-675.

- 774 [19] K. Snehal, B. B. Das, Acid, alkali and chloride resistance of binary, ternary and
775 quaternary blended cementitious mortar integrated with nano-silica particles, *Cem.*
776 *Concr. Compos.* 2021 104214.
- 777 [20] S. Sahoo, B. B. Das, S. Mustakim, Acid, alkali, and chloride resistance of concrete
778 composed of low-carbonated fly ash, *J. Mater. Civ. Eng.* 29 (3) (2017), 04016242.
- 779 [21] Z. Wei, G. Falzone, B. Wang, A. Thiele, G. Puerta-Falla, I. Pilon, N. Neithalath, G.
780 Sant, The durability of cementitious composites containing microencapsulated phase
781 change materials *Cem. Concr. Compos.* 81 (2017) 66-76.
- 782 [22] A. K. Suryavanshi, J. D. Scantlebury, S. B. Lyon, Mechanism of Friedel's salt
783 formation in cements rich in tri-calcium aluminate, *Cem. Concr. Res.* 26 (5) (1996)
784 717–727.
- 785 [23] K. Snehal, B.B. Das, M. Akanksha, Early age, hydration, mechanical and
786 microstructure properties of nano-silica blended cementitious composites, *Construct.*
787 *Build. Mater.* 233 (2020) 117212.
- 788 [24] S. Chithra, S.R.R.S. Kumar, K. Chinnaraju, The effect of colloidal nano-silica on
789 workability, mechanical and durability properties of high-performance concrete with
790 copper slag as partial fine aggregate, *Construct. Build. Mater.* 113 (2016) 794–804.
- 791 [25] H. Sattawa, T. Pulngern, S. Chucheeesakul, Effect of nanosilica particle size on the
792 water permeability, abrasion resistance, drying shrinkage, and repair work properties
793 of cement mortar containing nano-SiO₂, *Ann. Mater. Sci. Eng.* (2017).
- 794 [26] B. B Das, A. Mitra, Nanomaterials for construction engineering-A review, *Int. J. of*
795 *Mater. Mech. Manuf.* 2 (1) (2014) 41–46.
- 796 [27] H. Du, S. Du, X. Liu. Durability performance of concrete with Nano silica. *Constr.*
797 *Build. Mater.* 73 (2014) 705-712.
- 798 [28] ASTM C150/C150M - 15 Standard Specification for Portland Cement, ASTM
799 International, 2015.
- 800 [29] IS 383:2016 Coarse and Fine Aggregate for Concrete – Specification, Bureau of
801 Indian Standards, New Delhi, India.
- 802 [30] IS 4031 (Part 6) -1988, Determination of Compressive Strength of Hydraulic Cement
803 Other than Masonry Cement, Bureau of Indian Standards, New Delhi, India.
- 804 [31] M. Albitar, M. Mohamed Ali, P. Visintin, M. Drechsler, Durability evaluation of
805 geopolymer and conventional concretes *Constr, Build. Mater.* 136 (2017) 374–385.

- 806 [32] ASTM C490/C490M-17 Standard Practice for Use of Apparatus for the Determination
807 of Length Change of Hardened Cement Paste, Mortar, and Concrete, ASTM
808 International, 2017.
- 809 [33] ASTM C157/C157M-17 Standard Test Method for Length Change of Hardened
810 Hydraulic-Cement Mortar and Concrete, ASTM International, 2017.
- 811 [34] ASTM C1012/C1012M-18b Standard Test Method for Length Change of Hydraulic-
812 Cement Mortars Exposed to a Sulfate Solution, ASTM International, 2018.
- 813 [35] ASTM C596-18, Standard Test Method for Drying Shrinkage of Mortar Containing
814 Hydraulic Cement, ASTM International, 2018.
- 815 [36] W. Chen, B. Huang, Y. Yuan, M. Deng, Deterioration process of concrete exposed to
816 internal sulfate attack, *Materials*, 13 (2000) 1336.
- 817 [37] Z. Shi, M.R. Geiker, B. Lothenbach, K. De Weerd, S.F. Garzon, K.E. Rasmussen,
818 J. Skibsted, Friedel's salt profiles from thermogravimetric analysis and thermodynamic
819 modelling of Portland cement-based mortars exposed to sodium chloride solution,
820 *Cement Concr. Compos.* 78 (2017) 73–83.
- 821 [38] S. Barbhuiya, D. Kumala, D. Behaviour of a Sustainable Concrete in Acidic
822 Environment. *Sustainability*, 9 (2017) 1556.
- 823 [39] B. Tian, M. D. Cohen, Does gypsum formation during sulfate attack on concrete lead
824 to expansion? *Cem. Concr. Res.* 30(1) (2000) 117-123.
- 825 [40] A. M. Ramezani-pour, *Sulfate Resistance and Properties of Portland-Limestone*
826 *Cements, Thesis, University of Toronto, 2012.*
- 827 [41] E. F. Irassar, A. Di Maio, O. R. Batic, O. R. Sulfate attack on concrete with mineral
828 admixtures. *Cem. Concr. Res.* 26(1) (1995) 113-123.
- 829 [42] F. Kontoleon, P.E. Tsakiridis, A. Marinos, V. Kaloidas, M. Katsioti, influence of
830 colloidal nanosilica on ultrafine cement hydration: physicochemical and
831 microstructural characterization, *Constr. Build. Mater.* 35 (2012) 347–360.
- 832 [43] M. Drábik, L. Gálíková, E. Scholtzová, E. Hadzimová, Thermoanalytical events and
833 enthalpies of selected phases and systems of the chemistry and technology of concrete
834 part I. calcium-silicate-aluminate-sulfate hydrates, *Ceramics – Silikáty* 58 (3) (2014)
835 184-187.

836 [44] Black, L., Breen, C., Yarwood, J., Deng, C.-S., Phipps, J. Maitland, In situ Raman
837 analysis of hydrating C₃A and C₄AF pastes in presence and absence of sulfate. Adv.
838 Appl. Ceram. 1005 (4) (2006) 209-216.

839 [45] W. Kurdowski The protective layer and decalcification of c-s-h in the mechanism of
840 chloride corrosion of cement paste, Cem. Concr. Res. 34(9) (2004) 1555-155.

841 [46] A. Jayalath, R. Nicolas, M. Sofi, R. Shanks, T. Ngo, L. Ayea, P. Mendis, P. Properties
842 of cementitious mortar and concrete containing micro-encapsulated phase change
843 materials. Constr. Build. Mater. 120 (2016) 408–417.

844

845 **Highlights:**

- 846 • Formation of deleterious compounds such as Aft, Gy and Fs (due to the action of SO_4^{2-}
847 and Cl^- ions) amplified for PCM based cementitious mortar.
- 848 • Nano-silica (3%) modified PCM based cementitious mortar significantly reduced the
849 vulnerability to aggressive ions.
- 850 • Existence of endothermic peak at 250° C-300 °C indicates the presence of PCM (n-
851 octadecane) in nano-silica admixed mixes.
- 852 • Cross-linking action of PCM with tobermorite like C-S-H shifts the endothermic peak
853 from 80° C-300 °C to 250° C-300 °C.